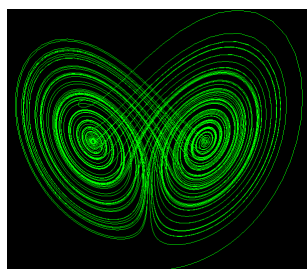


MASTER THESIS

Modelling for Science and Engineering

Numerical Study of L1-L2 Heteroclinic Connections between Invariant Tori in the Earth-Moon RTBP.

Miquel Barcelona Poza



October 2020

UAB

Universitat Autònoma de Barcelona

UNIVERSITAT AUTÒNOMA DE BARCELONA

Abstract

Master Degree in Modelling for Science and Engineering

Numerical Study of L1-L2 Heteroclinic Connections between Invariant Tori in the Earth-Moon RTBP

by Miquel Barcelona Poza

This project is devoted to the numerical computation of L1-L2 heteroclinic connections between invariant tori in the Earth-Moon circular, spatial restricted three-body problem (RTBP). For that purpose, we describe the parameterization method for invariant manifolds of fixed points of flows as an approach to estimate invariant manifolds. Specifically, we use this method to compute Taylor expansions of invariant manifolds around the libration points. After that, an error analysis is carried out for this semi-analytical technique and a range of energies of the Hamiltonian system. Finally, this method is applied to approximate the center-unstable and the center-stable manifold for both of the collinear equilibrium points as a final step to provide and estimate heteroclinic connections between invariant tori.

I would like to express my gratitude to my supervisor Dr. Josep-Maria Mondelo for his guidance, engagement and for the long dedicated hours through the learning process of this research work.

To my family for their support and continuous encouragement throughout my years of study.

And also to my flatmates. They know why.

Contents

Introduction	1
1 Preamble	5
1.1 Dynamical Systems	5
1.2 The Restricted Three-Body Problem	7
2 The Parameterization Method	11
2.1 Invariance Equation for Invariant Manifolds	11
2.2 Invariant Manifolds of Fixed Points	12
2.2.1 The Cohomological Equation	14
2.2.2 Styles of Parametrizations	16
2.3 Error Estimation	18
3 Accuracy tests of the invariant manifold expansions	21
3.1 Computation and Representation of the Center Manifold	21
3.1.1 Error Estimation	24
3.2 Computation of the Center-Stable and Center-Unstable Manifolds	26
3.2.1 Error Estimation	29
4 Numerical computation of heteroclinic connections	33
4.1 Determining Energies in Order to Look for Connections	34
4.2 Computation of Connections Between Tori	36
Conclusions	41
Appendices	
A Comments on the Implementation	45
Bibliography	47

Introduction

Homoclinic and heteroclinic connections of hyperbolic invariant sets represent a key part in the study of dynamical systems from a global point of view. In particular, astrodynamics constitute an important example of their applications. For instance, these connections play an essential role in mission design when a dynamical system is used to model the gravitational effect that the presence of external bodies has on a spacecraft. An important example of these situations is found on libration point (LP) missions, for which heteroclinic and homoclinic connections are used in order to connect in some way the vicinity of one or more libration points of a system.

One of the most relevant examples is found on Genesis Mission. This one was the first LP mission that used heteroclinic connections between objects around L_1 and L_2 libration points of the Sun-Earth system [1]. Whereas the LP mission called Artemis [2] used heteroclinic connections between L_1 and L_2 but in this case in an Earth-Moon system. The complexity and availability of the connections used for the design of LP missions are restricted because of the computational constraints that are usually imposed by the available methodology. The main motivation of this project is to contribute to develop a systematic way to find heteroclinic connections between the collinear libration points for a restricted three body problem (RTBP) system. The results that are included in this work are computed for the Earth-Moon RTBP, but the methodology can be exploited for different values of the mass parameter.

Some previous work related to the homoclinic and heteroclinic analysis in the RTBP has done before. The first results regarding homoclinic connections in a RTBP system are introduced in [3]. In this paper, the existence of homoclinic connections between planar Lyapunov orbits is theoretically proven for different values of the mass parameter. Later, some individual heteroclinic connections are computed numerically between different types of tori in [4]. The obtained heteroclinic connections are chosen in order to be interesting according to mission analysis. Further on, homoclinic connections of tori are computed in [5] for the spatial Hill's problem. The spatial Hill's problem is a particular approximation of the RTBP when the mass parameter is small enough. In 2007, the first description of all the heteroclinic connections between tori around L_1 and L_2 for a fixed energy level with astrodynamical interest is provided by [6] for the Hill's problem. Additionally,

heteroclinic connections between planar Lyapunov periodic orbits are found one by one in [7] and also by numerical continuation in [8]. Similar computations have been carried out during the last decades with different approaches. For instance, heteroclinic connections between pairs of libration points are computed in [9] with focus on mission design, but also theoretical results are obtained in [10], in this case they are oriented to compute scattering maps in the spatial Hill's problem.

In this work, we look for heteroclinic connections between tori around L_1 and L_2 by using the parameterization method to study the invariant manifolds associated to these libration points from the solution of invariance equation.

First, in Chapter 1 we present a theoretical basis and the main definitions of dynamical systems theory that will appear throughout the rest of the project. The system of differential equations that describe the dynamics of the RTBP is also presented together with some of its dynamical properties. The main notation that will be used in the following chapters is introduced in this part.

Chapter 2 is devoted to introduce the parameterization method as an approach to study invariant manifolds. The idea of this method is to seek for parameterization based on the solution of invariance equation, that are simplified through changes of variables that uses geometrical properties. The developments presented in this chapter follows the indications found in [14] and [15]. From the invariance equation and in order to obtain the Taylor expansions of invariant manifolds around fixed points of flows, the cohomological equation is presented. Therefore, different ways of solving this equation are introduced including a new style of parameterization called the mixed uncoupled style. Finally, several manners of determining the quality of the obtained expansions are presented.

Afterwards, in Chapter 3 it is used the parameterization method to represent the center manifold around the L_1 and L_2 libration points. The main goal of this part consist on performing an error analysis for the obtained expansions for the center manifold and also for the center-stable and center-unstable manifolds when the new style of parameterization is used. This error analysis allows to determine the domain of validity of the expansions in terms of energy and the order of computation.

Finally, in Chapter 4 an analysis of the heteroclinic connections between tori around L_1 and L_2 is carried out. This analysis uses the results from the previous chapter in order to delimit the error associated to the expansions. The new style of parameterization is applied, which is very useful when computing the center-stable and center-unstable manifolds. In this chapter, heteroclinic connections for the planar Lyapunov orbits are obtained and also four candidates of heteroclinic connections between invariant tori are found.

The numerical results presented in this work are firstly based on the software package available in <http://www.maia.ub.edu/dsg/param/>. This package includes routines to compute the expansions of invariant manifolds of fixed points as described in Chapter 2. However, some of these routines had to be adapted in order to introduce this new style of parameterization and some others had to be done from scratch. More information about the authorship of the used programs can be found in Appendix A.

Chapter 1

Preamble

The following chapter is devoted to present some of the key and necessary definitions and results that will be useful later through the developments and outcomes of the next chapters. Furthermore, we start to introduce the main notation that will be used later on throughout the project. We start by introducing what a dynamical system is and some of its properties and finally the restricted three body problem is introduced. The study of this problem will be the focus of the rest of the project.

1.1 Dynamical Systems

A dynamical system can be described as a way to define the evolution with time of any point in a given Euclidian space \mathcal{S} , that might be Euclidian or any other open subspace of an Euclidian one [11]. Due to the characteristics of our problem and for simplicity we can consider \mathcal{S} to be \mathbb{R}^n .

Consider $\mathbf{x} = (x_1, \dots, x_n)$ that denotes the state of a point. A dynamical system in \mathbb{R}^n describes the evolution of this state in terms of the time t . If time is measured only using integer time values, we talk about a *discrete dynamical system* which can be presented as the iteration of a function such as [11],

$$\mathbf{x}_{t+1} = f(\mathbf{x}_t), \quad t \in \mathbb{Z} \text{ or } \mathbb{N}. \quad (1.1)$$

In this case, the sub-index t is used to emphasize that the state of the system belongs to time t .

If time can be expressed in a continuous way with $t \in \mathbb{R}$, then we talk about a *continuous dynamical system*. In this scenario, the problem can be expressed using a system of

autonomous Ordinary Differential Equations,

$$\begin{cases} \dot{x}_1 = X_1(x_1, \dots, x_n) \\ \vdots \\ \dot{x}_n = X_n(x_1, \dots, x_n), \end{cases} \quad (1.2)$$

with $X_i: \mathbb{R}^n \rightarrow \mathbb{R}$ that are independent from time. Equation (1.2) can be described in a more compact way as,

$$\dot{\mathbf{x}} = \mathbf{X}(\mathbf{x}), \quad (1.3)$$

being $\mathbf{X}: \mathbb{R}^n \rightarrow \mathbb{R}^n$. From now on, we can consider that every time we talk about a dynamical system we will be referring to a continuous one.

In case the function \mathbf{X} is continuously differentiable and hence the system can be integrated for all $t \in \mathbb{R}$, it is possible to define a function called *time- t flow* or *t -map*, $\phi: \mathbb{R} \times \mathbb{R}^n \rightarrow \mathbb{R}^n$ with $t \in \mathbb{R}$. This function maps the state of \mathbf{x} to \mathbf{x}_t as the state after moving in time until t starting from \mathbf{x}_0 at t_0 . Therefore, the function is usually expressed like $\phi(t; t_0, \mathbf{x}_0)$. By introducing the notation $\phi_t(\mathbf{x}) := \phi(t; 0, \mathbf{x})$, with $\phi_t: \mathbb{R}^n \rightarrow \mathbb{R}^n$, the function can be stated in terms of the following initial value problem

$$\left. \begin{aligned} \frac{d}{dt} \phi_t(\mathbf{x}) &= \mathbf{X}(\phi_t(\mathbf{x})) \\ \phi_0(\mathbf{x}) &= \mathbf{x}, \end{aligned} \right\}, \quad (1.4)$$

where $\phi_t(\mathbf{x})$ can be thought as a \mathcal{C}^1 function in \mathbf{x} and t and it is continuous in the variable \mathbf{x} [11]. We can assume for the rest of the project that every dynamical system can be expressed in terms of the flow as in (1.4).

Let us introduce now some definitions regarding the flow sense and that will appear later on. Given an initial condition $\mathbf{x}_0 \in E \subset \mathbb{R}^n$, the function $\phi_t(\mathbf{x}_0): \mathbb{R} \rightarrow E$ with $t \in \mathbb{R}$ defines the *orbit* of the flow through the point \mathbf{x}_0 [11]. This trajectory through the initial condition defines a motion along the curve that can be expressed as the set

$$\gamma_{\mathbf{x}_0} = \{\mathbf{x} \in E \mid \mathbf{x} = \phi_t(\mathbf{x}_0), t \in \mathbb{R}\} \subset E. \quad (1.5)$$

In case this set is only made of by $\gamma_{\mathbf{x}_0} = \{\mathbf{x}_0\}$ then \mathbf{x}_0 is called a *fixed point* of the dynamical system and it also satisfies that $\mathbf{X}(\mathbf{x}_0) = 0$. Another particular case for the set $\gamma_{\mathbf{x}_0}$ is called *periodic orbit* with $T > 0$ being the *period*. In such a case, the flow must fulfill these two conditions: $\phi_T(\mathbf{x}) = \mathbf{x}$ and $\phi_t(\mathbf{x}) \neq \mathbf{x}$ for any $t < T$.

However, if one needs to think about a continuous dynamical system in a discrete way in order to simplify the complexity of a problem, it is possible to draw on to *Poincaré*

maps. Let's consider a dynamical system such as (1.3) and a differentiable and transversal hypersurface $\Sigma = \{\mathbf{x} \in U \mid g(\mathbf{x}) = 0\}$ to the vector field \mathbf{X} for all $\mathbf{x} \in \Sigma$. This means that the scalar product is $(\partial g / \partial \mathbf{x}) \cdot \mathbf{X}(\mathbf{x}) \neq 0$ for all $\mathbf{x} \in \Sigma$. This section is called the *Poincaré section*. Suppose that (1.3) has a periodic solution with period T denoted by $\phi_T(\mathbf{x}_0)$ satisfying that $\mathbf{x}_0 \in \Sigma$. Then, we can find an open subset U from Σ such that the orbits with initial conditions $\mathbf{y} \in U$ return to Σ in a certain time [11]. Then, the map that associates the points from U with the points corresponding to the first return to Σ is called *Poincaré map*. This map can be denoted by P in the following way:

$$\begin{aligned} P: U &\longrightarrow \Sigma \\ \mathbf{x} &\longmapsto \phi(\tau(\mathbf{x}), \mathbf{x}), \end{aligned} \tag{1.6}$$

where τ is the first time-return map of the point \mathbf{x} to the Poincaré section. In this way, thanks to Poincaré map, one can turn periodic orbits into fixed points such as $P(\mathbf{x}_0) = \mathbf{x}_0$ by construction.

We end this section by introducing the notion of invariant manifolds associated to dynamical systems. Let consider a set $S \subset \mathbb{R}^n$ such that S is an invariant set under the vector field \mathbf{X} from (1.3) if for any initial condition $\mathbf{x} \in S$ satisfies $\phi_t(\mathbf{x}) \in S$ for all $t \in \mathbb{R}$. In case that S has the structure of a differentiable manifold, then S is an invariant manifold [12].

We can distinguish two important types of invariant manifolds. These are the stable manifold and the unstable manifold. Let consider an invariant manifold S of initial conditions. Then we can denote by $W^s(S)$ (resp. $W^u(S)$) the stable manifold formed by a set of initial conditions such that their flows converges to the original set as $t \rightarrow +\infty$ (resp. $t \rightarrow -\infty$). In these terms, we can write

$$\begin{aligned} W^s(S) &= \{\mathbf{x} \in S \mid d(\phi_t(\mathbf{x}), S) \xrightarrow{t \rightarrow +\infty} 0\}, \\ W^u(S) &= \{\mathbf{x} \in S \mid d(\phi_t(\mathbf{x}), S) \xrightarrow{t \rightarrow -\infty} 0\}, \end{aligned} \tag{1.7}$$

where d denotes the Euclidian distance application in \mathbb{R}^n .

1.2 The Restricted Three-Body Problem

The *restricted three-body problem* (RTBP) describes the motion of a body with a neglected mass under the influence of two other bodies with masses m_1 and m_2 that are revolving around their center of mass in circular orbits. These two bodies are called *primaries* and they attract gravitationally the massless body while defining its motion. This problem

can be stated in terms of a dynamical system and it represents one of the most important and relevant application of the dynamical systems implemented to real life.

The problem is defined in \mathbb{R}^n with $n = 6$ and the massless body state is given by $\mathbf{x} = (x_1, \dots, x_6)$. The three first coordinates define the position of the body and they are denoted by (x, y, z) while the rest denote the mass momentum using as notation (p_x, p_y, p_z) . By performing a change of the coordinate system and choosing one that rotates with the primary bodies, it is possible to obtain a system where the two primaries are separated by only 1 unit of distance [13]. In that case, in terms of positions and momenta, the first primary is located at $(\mu, 0, 0, 0, \mu, 0)$ while the other one is fixed at $(\mu - 1, 0, 0, 0, \mu - 1, 0)$, being $\mu = m_2/(m_1 + m_2)$. In such a way, one can obtain a problem that can be described by the following Hamiltonian system

$$H(x, y, z, p_x, p_y, p_z) = \frac{1}{2}(p_x^2 + p_y^2 + p_z^2) - xp_y + yp_x - \frac{1 - \mu}{r_1} - \frac{\mu}{r_2}. \quad (1.8)$$

In this case, $r_1 = \sqrt{(x - \mu)^2 + y^2 + z^2}$ and $r_2 = \sqrt{(x - \mu + 1)^2 + y^2 + z^2}$ define the distances of the particle in study to the primary bodies. The value of H is commonly known as the energy of the body.

By taking this Hamiltonian, we can express this same problem in terms of a system of differential equations like (1.3) using that $\dot{q} = \partial H / \partial p_q$ and $\dot{p}_q = -\partial H / \partial q$ for $q \in \{x, y, z\}$. With that, one obtains a system in the form of (1.2) with

$$\begin{aligned} \dot{x}_1 &= p_x + y, & \dot{x}_4 &= p_y - \frac{1 - \mu}{r_1^3}(x - \mu) - \frac{\mu}{r_2^3}(x - \mu + 1), \\ \dot{x}_2 &= p_y - x, & \dot{x}_5 &= -p_x - \frac{1 - \mu}{r_1^3}y - \frac{\mu}{r_2^3}y, \\ \dot{x}_3 &= p_z, & \dot{x}_6 &= -\frac{1 - \mu}{r_1^3}z - \frac{\mu}{r_2^3}z. \end{aligned} \quad (1.9)$$

The RTBP has only 5 fixed points also known as *libration* points. They are denoted by L_i with $i \in \{1, \dots, 5\}$. On one hand, the two latest points L_4 and L_5 were discovered by Lagrange and they form an equilateral triangle with the primary ones. Their positions in the space are given by $(x, y, z) = (-1/2 + \mu, \mp\sqrt{3}/2, 0)$ respectively. While, on the other hand, the other three points were found by Euler and they are collinear with the primaries, so they have $y = z = 0$. The distance d_{L_j} for $j \in \{1, 2, 3\}$ for any of these libration points to the closest primary can be found by solving as the only real root of the Euler's quintic equation:

$$\begin{aligned} d_j^5 \mp (3 - \mu)d_j^4 + (3 - 2\mu)d_j^3 - \mu d_j^2 \pm 2\mu d_j - \mu &= 0, & j &= 1, 2 \\ d_j^4 + (2 + \mu)d_j^3 + (1 + 2\mu)d_j^2 - (1 - \mu)d_j^2 - 2(1 - \mu)d_j - (1 - \mu) &= 0 & j &= 3. \end{aligned} \quad (1.10)$$

With this equation, one can find the positions x_{L_j} on the x-axis for these fixed points and one can prove that is satisfied the condition given by

$$x_{L_2} < \mu - 1 < x_{L_1} < \mu < x_{L_3}. \quad (1.11)$$

This inequation tells us the relative locations of the fixed points respect to the primary bodies. More information about the properties of RTBP and its development can be found in [13].

Chapter 2

The Parameterization Method

In this chapter the main core of the project is presented. The parameterization method is an approach to obtain invariant manifolds of dynamical systems in the form of parameterizations, that are found by solving invariance equations which are first simplified through the use of geometrical properties. Its theoretical use leads to proofs of existence of invariant manifolds and its numerical application leads to the actual computation of high order approximations of these manifolds.

In this case, only continuous dynamical systems will be considered as the final goal is to use this method for the computation of invariant manifolds around fixed points of vector fields. Particularly, it will be applied to the Earth-Moon RTBP to compute approximations of the center-stable and the center-unstable manifolds around the collinear libration points L_1 and L_2 . Note that this includes the invariant stable and unstable manifolds of all the invariant objects (such as periodic orbits and tori) inside the center manifold.

The chapter begins by defining the invariance equation for flows of continuous dynamical systems and it follows by solving the equation using Taylor expansions around fixed points of the system. In this way, the cohomological equation is introduced. The chapter ends by presenting different ways of solving this equation and how to quantify the associated error to these expansions. The contents explained below follow the theoretical explanations and developments from [14, 15].

2.1 Invariance Equation for Invariant Manifolds

Let \mathcal{U} be the phase space where a dynamical system described by a vector field X is defined. Then, the vector field is defined like $X : \mathcal{U} \rightarrow \mathcal{U}$ and generates a continuous dynamical system on the manifold \mathcal{U} . The action of this system on the given manifold is denoted by the local coordinates $x \in \mathcal{U}$ and it is also considered a system of differential equations given by $\dot{x} = X(x)$. Let denote by $\Phi_t(x)$ the time- t flow associated to this dynamical system.

Assume $\mathcal{F} \subset \mathcal{U}$ is a submanifold that can be described by an injective immersion $W : \mathcal{V} \rightarrow \mathcal{U}$. In this case, W defines a parameterization of the submanifold \mathcal{F} by $\mathcal{F} = W(\mathcal{V})$. Let suppose there exists a vector field $f : \mathcal{V} \rightarrow \mathcal{V}$ with \mathcal{V} being its ambient space that describes the internal dynamics on the submanifold \mathcal{V} by $\dot{s} = f(s)$, where s are the local coordinates on \mathcal{V} . In the same way as before, the internal flow on \mathcal{V} can be denoted by $\phi_t(s)$.

Then, the submanifold \mathcal{F} parameterized by W is said to be X-invariant if it satisfies the following equation

$$\Phi_t(W(s)) = W(\phi_t(s)). \quad (2.1)$$

The idea of the above equation is that given an initial condition s in the submanifold \mathcal{F} , the result of taking his image in the phase space \mathcal{U} and integrating it until a time t using the flow Φ_t , must be the same as integrating in the submanifold using the internal flow ϕ_t and then calculate its image in \mathcal{U} through the parameterization W .

This equation can be differentiated at $t = 0$ by using the definition provided in (1.4). In this way, one obtains the infinitesimal version of the invariance equation for invariant manifolds described by the parameterization W as

$$X(W(s)) = DW(s)f(s). \quad (2.2)$$

2.2 Invariant Manifolds of Fixed Points

In this section we would like to a compute d -dimensional manifold that contains a fixed point \mathbf{p} from a vector field $\dot{\mathbf{x}} = \mathbf{X}(\mathbf{x})$, with $\mathbf{X} : \mathbb{R}^n \rightarrow \mathbb{R}^n$ defining a n -dimensional continuous dynamical system, and it is tangent to a d -dimensional eigenspace of the differential of \mathbf{X} and invariant by the flow. For that purpose, one have to solve the invariance equation (2.2) by using changes of variables and some manipulations.

Consider \mathbf{p} the fixed point of the system $\dot{\mathbf{x}} = \mathbf{X}(\mathbf{x})$ satisfying that $\mathbf{X}(\mathbf{p}) = 0$. Assume that the differential of the vector field $D\mathbf{X}$ evaluated at the fixed point has the set of eigenvalues denoted by

$$\text{Spec}D\mathbf{X} = \{\lambda_1, \dots, \lambda_n\}, \quad \lambda_i \in \mathbb{C} \quad \forall i = 1, \dots, n, \quad (2.3)$$

and each one of these eigenvalues has associated an eigenvector denoted by $\mathbf{v}_i \in \mathbb{C}^n$ for each λ_i . Let's denote by $\Phi_t(\mathbf{x})$ the associated flow to this system.

Taking all of this into account, one can define the matrix $\mathbf{P} \in \mathbb{C}^{n \times n}$ composed by the eigenvectors such like $\mathbf{P} = (\mathbf{v}_1, \dots, \mathbf{v}_n)$. This matrix can be used to determine the change

of variables given by

$$\mathbf{x} = \mathbf{p} + \mathbf{P}\mathbf{y}, \quad \mathbf{y} = (y_1, \dots, y_n)^\top \in \mathbb{R}^n. \quad (2.4)$$

This change defines an equivalent dynamical system given by the vector field $\mathbf{Y} : \mathbb{R}^n \rightarrow \mathbb{R}^n$ with $\dot{\mathbf{y}} = \mathbf{Y}(\mathbf{y})$. From the previous definitions, this system can be written as

$$\dot{\mathbf{y}} = \mathbf{Y}(\mathbf{y}) = \mathbf{P}^{-1}\mathbf{X}(\mathbf{p} + \mathbf{P}\mathbf{y}), \quad (2.5)$$

and then it satisfies that $\mathbf{Y}(\mathbf{0}) = \mathbf{0}$, so the origin is a fixed point of the new dynamical system. In the same way, by using the chain rule, one can see that the differential of the vector field evaluated at this fixed point fulfills that

$$D\mathbf{Y}(\mathbf{y})|_{\mathbf{y}=\mathbf{0}} = \mathbf{P}^{-1}D\mathbf{X}(\mathbf{p} + \mathbf{P}\mathbf{y})|_{\mathbf{y}=\mathbf{0}} = \mathbf{P}^{-1}D\mathbf{X}(\mathbf{p})\mathbf{P} = \text{diag}\{\lambda_1, \dots, \lambda_n\} = \mathbf{M},$$

by definition of \mathbf{P} . Then, by Taylor expansions, the system can be approximated by $\dot{\mathbf{y}} = \mathbf{M}\mathbf{y} + \mathcal{O}(\|\mathbf{y}\|^2)$, being \mathbf{M} the diagonal matrix composed by the eigenvalues of the differential of \mathbf{X} at \mathbf{p} .

As we can see, our initial problem has turned out into the computation of an expansion of a d -dimensional manifold that contains the origin, invariant by the flow associated to \mathbf{Y} , and is tangent to the y_1, \dots, y_d coordinates as the eigenspace of interest is defined by the set $\{\mathbf{y} \in \mathbb{R}^n \mid y_{d+1} = \dots = y_n = 0\}$.

So a parameterization of a manifold satisfying the above conditions is looked for and it is denoted by $\mathbf{W} : \mathbb{C}^d \rightarrow \mathbb{C}^d$ with $d \leq n$. The internal dynamics in the manifold are described by the dynamical system given by the differential equation $\dot{\mathbf{s}} = \mathbf{f}(\mathbf{s})$ with $\mathbf{f} : \mathbb{C}^d \rightarrow \mathbb{C}^d$ and $\mathbf{s} \in \mathbb{C}^d$ being the local coordinates in the manifold. The flow associated to internal dynamics is denoted by $\phi_t(\mathbf{s})$.

Then, our goal is to find the expressions of the functions \mathbf{f} and \mathbf{W} . For that reason, it is necessary to solve the invariance equation given by (2.2) and, in this particular case, can be written as

$$\mathbf{Y}(\mathbf{W}(\mathbf{s})) = D\mathbf{W}(\mathbf{s})\mathbf{f}(\mathbf{s}). \quad (2.6)$$

The parameterization given by \mathbf{W} and the internal dynamics \mathbf{f} that are obtained by solving the above equation are related with the \mathbf{y} coordinates described by the change in (2.4). If one would want to recover the original system described by the \mathbf{x} coordinates and obtain the parametrization $\bar{\mathbf{W}}$ of the manifold in the original system of coordinates

is necessary to undo the change by taking

$$\bar{\mathbf{W}}(s) = \mathbf{p} + \mathbf{P}\mathbf{W}(s). \quad (2.7)$$

2.2.1 The Cohomological Equation

The goal of this section is to compute approximations of the functions \mathbf{W} and \mathbf{f} that solve the invariance equation given by (2.6). For that purpose, we consider the expansions of them in power series such like

$$\mathbf{W} = \sum_{k \geq 0} \mathbf{W}_k, \quad \mathbf{f} = \sum_{k \geq 0} \mathbf{f}_k. \quad (2.8)$$

In either case, each one of the summands is a vector of homogeneous polynomials of degree k defined in the $\mathbf{s} = (s_1, \dots, s_d)^\top$ coordinates associated to the dynamics reduced to the invariant manifold. On the one hand, \mathbf{W}_k is an n -vector of this polynomials, while on the other hand, \mathbf{f}_k is a d -dimensional vector. Taking everything into account, each component can be written as follows

$$\begin{aligned} \mathbf{W}_k &= (W_k^1, \dots, W_k^n)^\top, & W_k^i &= \sum_{m_1 + \dots + m_d = k} W_{k,m}^i s_1^{m_1} \dots s_d^{m_d} \\ \mathbf{f}_k &= (f_k^1, \dots, f_k^d)^\top, & f_k^i &= \sum_{r_1 + \dots + r_d = k} f_{k,r}^i s_1^{r_1} \dots s_d^{r_d}, \end{aligned} \quad (2.9)$$

with $(m_1, \dots, m_d), (r_1, \dots, r_d) \in \mathbb{N}^d$.

With this assumption, one can solve the invariance equation for \mathbf{W} and \mathbf{f} by solving it order by order

$$\mathbf{Y}(\mathbf{W}(s))|_k = D\mathbf{W}(s)\mathbf{f}(s)|_k, \quad (2.10)$$

in this case $|_k$ denotes the part of the Taylor series that is an homogeneous polynomial of degree k .

First of all, in order to satisfy the properties imposed by the definition of the parametrization, one can defined the two first orders. On the one hand, the independent terms of both \mathbf{W}_0 and \mathbf{f}_0 must be

$$\mathbf{W}_0 = \mathbf{0}, \quad \mathbf{f}_0 = \mathbf{0}, \quad (2.11)$$

because of the manifold has to contain the fixed point and then the invariance equation must be satisfied.

On the other hand, one have to assure that the manifold is tangent to the d -dimensional eigenspace characterized by the first d -variables. In these terms, it is only necessary to

take the first degree of the parametrization as

$$\mathbf{W}_1 = (s_1, \dots, s_d, 0, \dots, 0). \quad (2.12)$$

With that, and applying a Taylor expansion around the fixed point of the vector field \mathbf{Y} to the invariance equation, the value of \mathbf{f} at first order will be deduced from

$$\mathbf{Y}(\mathbf{W}(\mathbf{s}))|_1 = \mathbf{Y}(0) + D\mathbf{Y}(0)D\mathbf{W}(0)|_0 \mathbf{s} + \mathcal{O}(\|\mathbf{s}\|^2) = \mathbf{M} \begin{pmatrix} I_{d \times d} \\ 0 \end{pmatrix} \mathbf{s} + \mathcal{O}(\|\mathbf{s}\|^2)$$

then, as $\mathbf{f}_0 = \mathbf{0}$, the first order must satisfy that

$$\mathbf{f}_1 = (\lambda_1 s_1, \dots, \lambda_d s_d, 0, \dots, 0)^\top \quad (2.13)$$

Then, assuming that at each order k the values of $\mathbf{W}_{<k} = \mathbf{W}_0 + \dots + \mathbf{W}_{k-1}$ and $\mathbf{f}_{<k} = \mathbf{f}_0 + \dots + \mathbf{f}_{k-1}$ are known, we can construct an iterative method to solve the invariance equation at each order k . By taking the left hand side in (2.10) and applying a Taylor expansion at the fixed point, one obtains the expression

$$\begin{aligned} \mathbf{Y}(\mathbf{W}(\mathbf{s}))|_k &= \mathbf{Y}(\mathbf{W}_{\leq k})|_k = \mathbf{Y}(\mathbf{W}_{<k} + \mathbf{W}_k)|_k = \mathbf{Y}(\mathbf{W}_{<k})|_k + D\mathbf{Y}(\mathbf{W}_{<k})\mathbf{W}_k + \mathcal{O}_{>k} \\ &= \mathbf{Y}(\mathbf{W}_{<k})|_k + D\mathbf{Y}(0)\mathbf{W}_k + \mathcal{O}_{>k}, \end{aligned}$$

where for the sake of simplicity, the evaluation at the reduced coordinates \mathbf{s} has been omitted. Now, this expression must satisfy the right hand side of the same equation (2.10). If we compute the order k at the right hand side by applying that the differential of the parametrization \mathbf{W} at order k reduces its order by 1, one obtains the following expression

$$\begin{aligned} D\mathbf{W}(\mathbf{s})\mathbf{f}(\mathbf{s})|_k &= D\mathbf{W}_{\leq k}\mathbf{f}_{\leq k}|_k = \sum_{l=1}^k D\mathbf{W}_{k-l+1}\mathbf{f}_l \\ &= D\mathbf{W}_1\mathbf{f}_k + \sum_{l=2}^{k-1} D\mathbf{W}_{k-l+1}\mathbf{f}_l + D\mathbf{W}_1\mathbf{f}_k. \end{aligned}$$

Taking these two expressions together and putting all the known terms at the right hand side of the equation and the rest at the left hand side, we obtain

$$D\mathbf{Y}(0)\mathbf{W}_k - D\mathbf{W}_k\mathbf{f}_1 - D\mathbf{W}_1\mathbf{f}_k = -\mathbf{R}_k,$$

where \mathbf{R}_k is the right hand side of the equation and contains all the known terms. It can be expressed by

$$\mathbf{R}_k = \mathbf{Y}(\mathbf{W}_{<k})|_k - \sum_{l=2}^{k-1} D\mathbf{W}_{k-l+1} \mathbf{f}_l. \quad (2.14)$$

Then, if we apply the properties at orders 0 and 1 for \mathbf{f} and \mathbf{W} and the definition of $D\mathbf{Y}(\mathbf{0})$, it is possible to express the above equation in terms of the coefficients of each one of the homogeneous polynomials at order k by

$$\begin{aligned} (\langle \bar{\lambda}, m \rangle - \lambda_i) W_{k,m}^i + f_{k,m}^i &= R_{k,m}^i, & i \in \{1, \dots, d\}, \\ (\langle \bar{\lambda}, m \rangle - \lambda_i) W_{k,m}^i &= R_{k,m}^i, & i \in \{d+1, \dots, n\}, \end{aligned} \quad (2.15)$$

where $\bar{\lambda}$ is defined as $\bar{\lambda} = (\lambda_1, \dots, \lambda_d)$. Then, $\langle \bar{\lambda}, m \rangle$ is the dot product between $\bar{\lambda}$ and $m = (m_1, \dots, m_d)$ the vector of the exponents of each s_j for the component i of the parametrization \mathbf{W} at order k .

The equation (2.15) is known as the cohomological equation at order k and it gives us an expression to compute the values of the manifold and the vector field of the internal dynamics at order k .

2.2.2 Styles of Parametrizations

The cohomological equation in (2.15) can be solved for the manifold provided that there are no cross-resonances for $i \in \{d+1, \dots, n\}$. This means that it has to be satisfied that $\lambda_i \neq \langle \bar{\lambda}, m \rangle$ for any $i \in \{d+1, \dots, n\}$. The solution of the equation for $i \in \{1, \dots, d\}$ can be computed in many different ways. That is why there are different styles of parametrization depending on the chosen strategy to solve the cohomological equation.

The Graph Style

The graph style is the simplest way to solve the cohomological equation. In this case, one chooses

$$\begin{aligned} W_{k,m}^i &= 0, & f_{k,m}^i &= R_{k,m}^i, & i \in \{1, \dots, d\}, \\ W_{k,m}^i &= \frac{R_{k,m}^i}{\langle \bar{\lambda}, m \rangle - \lambda_i}, & & & i \in \{d+1, \dots, n\}. \end{aligned} \quad (2.16)$$

This choice ensure to overcome any internal resonance in the d first coordinates of the manifold. An internal resonance takes place when $\langle \bar{\lambda}, m \rangle - \lambda_i = 0$ for $i = 1, \dots, d$. It is called internal because λ_i is one of the components in $\bar{\lambda}$. While a cross resonance occurs when $\langle \bar{\lambda}, m \rangle - \lambda_i = 0$ when $i = d+1, \dots, n$.

Hence, the manifold in those coordinates is given by the defined first order of \mathbf{W} , being $W^1(\mathbf{s}) = s_1, \dots, W^d(\mathbf{s}) = s_d$. This method is called graph style because it defines a graph respect to the variables (s_1, \dots, s_d) .

The Normal Form Style

The normal style consists on taking $f_{k,m}^i = 0$ when there is no internal resonances. If not, in order to overcome the problem, $W_{k,m}^i$ is taken as null. In such a case, the choice of the solution is given by

$$\begin{aligned} W_{k,m}^i &= 0, & f_{k,m}^i &= R_{k,m}^i, & \text{if } \lambda_i &= \langle \bar{\lambda}, m \rangle, \\ W_{k,m}^i &= \frac{R_{k,m}^i}{\langle \bar{\lambda}, m \rangle - \lambda_i}, & f_{k,m}^i &= 0, & \text{otherwise.} \end{aligned} \quad (2.17)$$

The Mixed Style

Sometimes it is useful to use an intermediate strategy between the graph style and the normal form style. These kind of strategies are known as mixed styles and they are used to reveal the existence of invariant submanifolds in the reduced space.

Suppose that given the set of indexes $I_1, \dots, I_L \subset \{1, \dots, d\}$ we want the submanifolds formed by $V_i = \{s_j = 0 \mid \forall j \in I_i\}$ for $i = 1, \dots, L$ to be invariant by the reduced dynamics described by $\dot{\mathbf{s}} = \mathbf{f}(\mathbf{s})$. Without lose of generality, let us consider a set given by I_1 with $V_1 = \{s_i = 0 \mid i \in I_1\}$ and the same argument is valid for the remaining set of indexes. The reduced dynamics in parameter space can be written as

$$\begin{cases} \dot{s}_1 &= f^1(s_1, \dots, s_d), \\ \vdots & \\ \dot{s}_d &= f^d(s_1, \dots, s_d). \end{cases} \quad (2.18)$$

Then, to make sure that the vector field $\dot{\mathbf{s}} = \mathbf{f}(\mathbf{s})$ leaves invariant the set V_1 it is sufficient that $f^j(s_1, \dots, s_d) = 0$ for any \mathbf{s} such that $s_j = 0$ for all $j \in I_1$. Given a j in I_1 , to satisfy this condition we need that

$$f_k^j(\mathbf{s}) = \lambda_j s_j + \sum_{|m|=2}^{\infty} f_{k,m} m^j s_1^{m_1} \dots s_d^{m_d} = 0, \quad j \in I_1.$$

But, if \mathbf{s} fulfills that $s_i = 0$ for all $i \in I_i$, then the only summands that are not canceled in the above equation are those that have $m_i = 0$ for all $i \in I_1$. Therefore, if we ask the corresponding factors to be $f_{k,m}^j = 0$, then $f_k^j(\mathbf{s}) = 0$.

This means that, when the mixed style is used for a given set of indexes I_1, \dots, I_L , the cohomological equation in (2.15) is solved by choosing

$$\begin{aligned} W_{k,m}^i &= \frac{R_{k,m}^i}{\langle \bar{\lambda}, m \rangle - \lambda_i}, & f_{k,m}^i &= 0, & \text{if } \exists l : i \in I_l \text{ and } m_j = 0 \forall j \in I_l, \\ W_{k,m}^i &= 0, & f_{k,m}^i &= R_{k,m}^i, & \text{otherwise.} \end{aligned} \quad (2.19)$$

This method can only be applied if $\langle \bar{\lambda}, m \rangle - \lambda_j \neq 0$ for all $m \in \mathbb{N}^d$ with $m_i = 0$ for all i in any I_l , $l = 1, \dots, L$.

The Mixed Uncoupled Style

In some cases (as in the one presented in the next chapter), it is useful to have the first $d - 1$ differential equations of the reduced dynamics uncoupled from the last one. This is to have a system of ODE for the reduced dynamics such as

$$\begin{cases} \dot{s}_1 &= f^1(s_1, \dots, s_{d-1}), \\ \vdots & \\ \dot{s}_{d-1} &= f^{d-1}(s_1, \dots, s_{d-1}), \\ \dot{s}_d &= f^d(s_1, \dots, s_{d-1}, s_d). \end{cases} \quad (2.20)$$

This means that the first $d - 1$ components of the reduced flow are independent of the last component of the initial condition. This is, the first $d - 1$ components of $\phi_t(s_1, \dots, s_{d-1}, s_d)$ and $\phi_t(s_1, \dots, s_{d-1}, 0)$ are equal. In order to impose the condition in (2.20), since

$$f_k^j(\mathbf{s}) = \lambda_j s_j + \sum_{|m|=2}^{\infty} f_{k,m}^j s_1^{m_1} \dots s_d^{m_d}, \quad j = 1, \dots, d - 1, \quad (2.21)$$

it is sufficient that, if $m_d \neq 0$, we choose $f_{k,m}^i = 0$ and $W_{k,m}^i = R_{k,m}^i / (\langle \bar{\lambda}, m \rangle - \lambda_i)$. Again this method can only be applied when $\lambda_i - \langle \bar{\lambda}, m \rangle \neq 0$ when $f_{k,m}^i$ needs to be zero.

2.3 Error Estimation

When the parameterization method is applied to compute numerical approximations of the internal dynamics and the parameterization of the manifold, an error estimation is needed in terms of evaluating the quality of the obtained expansions for \mathbf{W} and \mathbf{f} . Assuming that these two expressions are computed up to a maximum order k_{max} , then

we will have the truncated expansions given by

$$\mathbf{W}_{k \leq k_{max}} := \mathbf{W}_1 + \mathbf{W}_2 + \cdots + \mathbf{W}_{k_{max}}, \quad \mathbf{f}_{k \leq k_{max}} := \mathbf{f}_1 + \mathbf{f}_2 + \cdots + \mathbf{f}_{k_{max}}.$$

For the sake of notation simplicity, let's denote by \mathbf{W} and \mathbf{f} these two truncated power series for the rest of the project.

Let's take \mathbf{s}_0 as an initial condition in parameter space, then it is fulfill that $\phi_0(\mathbf{s}_0) = \mathbf{s}_0$ and $\bar{\mathbf{W}}(\mathbf{s}_0) = \Phi_0(\bar{\mathbf{W}}(\mathbf{s}_0))$ in terms of the corresponding parameterization of the manifold in the original variables given by the \mathbf{x} coordinates. Then, by choosing an integration time T that will depend on the study under consideration, we will have the following ways to determine the numerical error associated to the expansion:

- **Error in the invariance equation.** By definition of the parameterization method, the obtained expressions should satisfy the invariance equation given by (2.6). Then, this expression becomes a useful method to estimate the deviation of the estimated expansions by computing

$$e_I(T, \mathbf{s}_0) = \sup_{t \in [0, T]} \left\| \mathbf{X}(\bar{\mathbf{W}}(\phi_t(\mathbf{s}_0))) - D\bar{\mathbf{W}}(\phi_t(\mathbf{s}_0))\mathbf{f}(\phi_t(\mathbf{s}_0)) \right\|. \quad (2.22)$$

- **Error in the orbit.** The parameterization of the manifold must satisfy the condition expressed by (2.1). This means that integrating up to time T using original coordinates must be equal to integrate until T in parameter space and computing the image in original space through the parameterization \mathbf{W} . This gives us a way to estimate the error by computing

$$e_O(T, \mathbf{s}_0) = \sup_{t \in [0, T]} \left\| \bar{\mathbf{W}}(\phi_t(\mathbf{s}_0)) - \Phi_t(\bar{\mathbf{W}}(\mathbf{s}_0)) \right\|. \quad (2.23)$$

- **Error in the reduced first integral H .** Assuming that the system $\dot{\mathbf{x}} = \mathbf{X}(\mathbf{x})$ can be written in a hamiltonian form given by $H(\mathbf{x})$, then the value of H must be constant through an orbit characterized by an initial value \mathbf{x}_0 . Then, this same behavior should be preserved when integrating in parameter space and then its image in the original space is computed through the parameterization. Taking this into account, another way of estimating the error is given by

$$e_H(T, \mathbf{s}_0) = \sup_{t \in [0, T]} \left\| H(\bar{\mathbf{W}}(\phi_t(\mathbf{s}_0))) - H(\bar{\mathbf{W}}(\mathbf{s}_0)) \right\|. \quad (2.24)$$

For the rest of the chapters, we will refer to the error in the orbit every time we talk about the error made in the computation of expansions. This error is the most relevant

from the point of view of the applications.

Chapter 3

Accuracy tests of the invariant manifolds expansions around the $L_{1,2}$ collinear points of the Earth-Moon RTBP

In this chapter we present two examples of manifold computations using the parametrization method explained in the last chapter. We first apply this method to compute the center manifold of L_1 and L_2 of the RTBP for the Earth-Moon mass parameter μ . Later, the same method is applied to compute the center-stable and center-unstable manifolds of L_1 and L_2 respectively for the same problem. In order to do that, two styles of parametrization are used: the mixed style and a mixed uncoupled style. A representation of the computational error depending on the order of the computed expansions is done. This representation allows us to determine the range of validity of each expansion in terms of the degree and the energy of the manifold.

3.1 Computation and Representation of the Center Manifold

We first start by computing and representing the center manifold W^c of L_1 and L_2 of the Earth-Moon RTBP as a 4-dimensional manifold of a 6-dimensional dynamical system using the mixed style. This means that in our case, $d = 4$ and $n = 6$ and then the parameterization of $W^c(L_{1,2})$ is¹ $\mathbf{W} : \mathbb{R}^4 \rightarrow \mathbb{R}^6$. Let's denote by $\dot{\mathbf{x}} = \mathbf{X}(\mathbf{x})$ the system of ODE that represents the vector field associated to the Earth-Moon RTBP given by (1.9).

¹The parameterization \mathbf{W} is defined in a neighborhood of 0 and its size is determined by the accuracy tests.

The eigenvalues of $D\mathbf{X}(L_{1,2})$ have the following form:

$$\text{Spec}D\mathbf{X}(L_{1,2}) = \{i\omega_p, -i\omega_p, i\omega_v, -i\omega_v, \lambda, -\lambda\}, \quad (3.1)$$

with $\lambda \in \mathbb{R}$ and $\omega_p, \omega_v, \lambda > 0$. Note that we have include the sub-indexes p and v to indicate the direction of the eigenvectors \mathbf{u}_p and \mathbf{u}_v associated to the eigenvalues $\pm i\omega_p$ and $\pm i\omega_v$. In each case, p means planar as the eigenplane spanned by the vectors $\bar{\mathbf{u}}_p$ and $\bar{\mathbf{u}}_p$ has components $z = p_z = 0$ while v denotes vertical as the eigenplane corresponding to eigenvalues $\pm i\omega_v$ has only the vertical components non-zero ($x = y = p_x = p_y = 0$). Taking (3.1) into account, the linear behavior around the L_1 and L_2 points is of the type center \times center \times saddle [14]. Therefore, by the Lyapunov's Center Theorem, one can ensure that each center gives rise to a family of periodic orbits named planar and vertical and they are part of the center manifold of the fixed point $L_{1,2}$ [14].

In this way, if one wants to compute the corresponding center manifold W^c by using the parameterization method it is sufficient to choose as d the d first coordinates of \mathbf{X} that generate that center manifold. Hence, the obtained parameterization \mathbf{W} contains $L_{1,2}$ and it is tangent to the d -dimensional eigenspace of $D\mathbf{X}(L_{1,2})$ spanned by the eigenvectors of $\pm i\omega_v$ and $\pm i\omega_p$ by construction and therefore, this parameterization corresponds to the center manifold by definition of this one.

Taking everything into account, we will proceed by applying the change of coordinates in (2.4). By doing this, the dynamical system under study turns out to be

$$\mathbf{Y}(\mathbf{y}) := \mathbf{P}^{-1}(\mathbf{X}(L_{1,2} + \mathbf{P}\mathbf{y})), \quad (3.2)$$

where \mathbf{P} is the matrix that has as columns de eigenvectors of $\pm i\omega_p$, $\pm i\omega_p$ and $\pm\lambda$ in that order. This change allows us to compute the center manifold of the system expressed in y coordinates by using the parameterization method explained in Chapter 2. The method will give a parameterization \mathbf{W} and the reduced vector field \mathbf{f} . In this way, by applying the following change

$$\bar{\mathbf{W}}(\mathbf{s}) = L_{1,2} + \mathbf{P}\mathbf{W}(\mathbf{s}), \quad (3.3)$$

one can obtain a parameterization of the 4D center manifold of $L_{1,2}$ in the original system of coordinates.

To compute the parameterization of the center manifold $W^c(L_{1,2})$ we choose the mixed style with $L = 2$ and a set of indexes formed by $I_1 = \{1, 2\}$ and $I_2 = \{3, 4\}$. This choice is numerically found to be free of resonances². Therefore, this ensures that $\{\bar{\mathbf{W}}(s_1, s_2, 0, 0)\}_{s_1, s_2}$ will describe the 2D manifold spanned by the family of the planar Lyapunov orbits,

²This is also a requirement for the application of the Lyapunov's Center Theorem.

whereas $\{\bar{W}(0, 0, s_3, s_4)\}_{s_3, s_4}$ describes the 2-dimensional manifold corresponding to the vertical Lyapunov orbits. Once the parameterization is computed, our goal is to represent Poincaré sections at $\Sigma_h = \{s_4 = 0\}$ of iso-energetic slices of the center manifold being h the energy level. This means that since W^c is a 4-dimensional manifold, these slices are 2D and then they can be represented on a plane as in Figure 3.1.

Given an energy level h and a Poincaré section described by $\Sigma_h = \{s_4 = 0\}$, we know that there is only one planar Lyapunov orbit, which in parameter space is given by points of the form $(s_1, s_2, 0, 0)$ for some s_1 and s_2 values. Then, if one considers an initial condition of the form $(0, s_2, 0, 0)$, it is possible to adjust s_2 in order to obtain the given energy level. Then, by integrating in the reduced space using the computed expansion for $\mathbf{f}(\mathbf{s})$, the external curves in Figure 3.1 are obtained. The rest of points in the Poincaré section of the iso-energetic slice in the center manifold are all univocally defined by the components (s_1, s_2) as $s_4 = 0$ and the s_3 component is obtained from the energy. By numerical computation, it is found that if we start at a point (s_1, s_2) that is outside the region bounded by the planar Lyapunov orbit it is not possible to find any s_3 that satisfies the given energy. This same behavior can be appreciated when these plots are computed by using linear approximations [16]. Therefore, all the points in the Poincaré section of the iso-energetic slice are bounded by the planar Lyapunov orbit. In particular, the point with $s_1 = s_2 = 0$ corresponds to the vertical Lyapunov orbit.

In order to represent the dynamics inside that curve we take equally spaced initial conditions over the s_2 axis and we compute the s_3 value from the energy. This is taking initial conditions of the form $(0, s_2, s_3, 0)$ with $(0, s_2)$ inside the region bounded by the outer curve. Then, we can integrate each one of these initial conditions numerically using the computed expansion for $\mathbf{f}(\mathbf{s})$ to finally represent a number of Poincaré sections large enough in order to fill a curve inside the bounded region. In this way, we obtain all the interior points in Figure 3.1. These invariant closed curves inside the region bounded by the planar Lyapunov orbit correspond to the intersections of the 2D invariant tori of $W^c(L_{1,2})$ at the fixed energy with the Poincaré section Σ_h . A more exhaustive numerical exploration (that would also be computationally more costly) would also reveal periodic orbits, secondary tori in an island chain structure and even chaotic dynamics.

In Table 3.1 we present the computing times that are necessary to obtain the points from one of the plots in Figure 3.1 by integrating numerically the obtained expansion for the reduced vector field. We get these times from the computation of iso-energetic slices at $h = -1.585$ for $W^c(L_2)$ at several orders of computation by taking 50 initial conditions over the s_2 axis and for each one of these points 100 of Poincaré sections are computed.

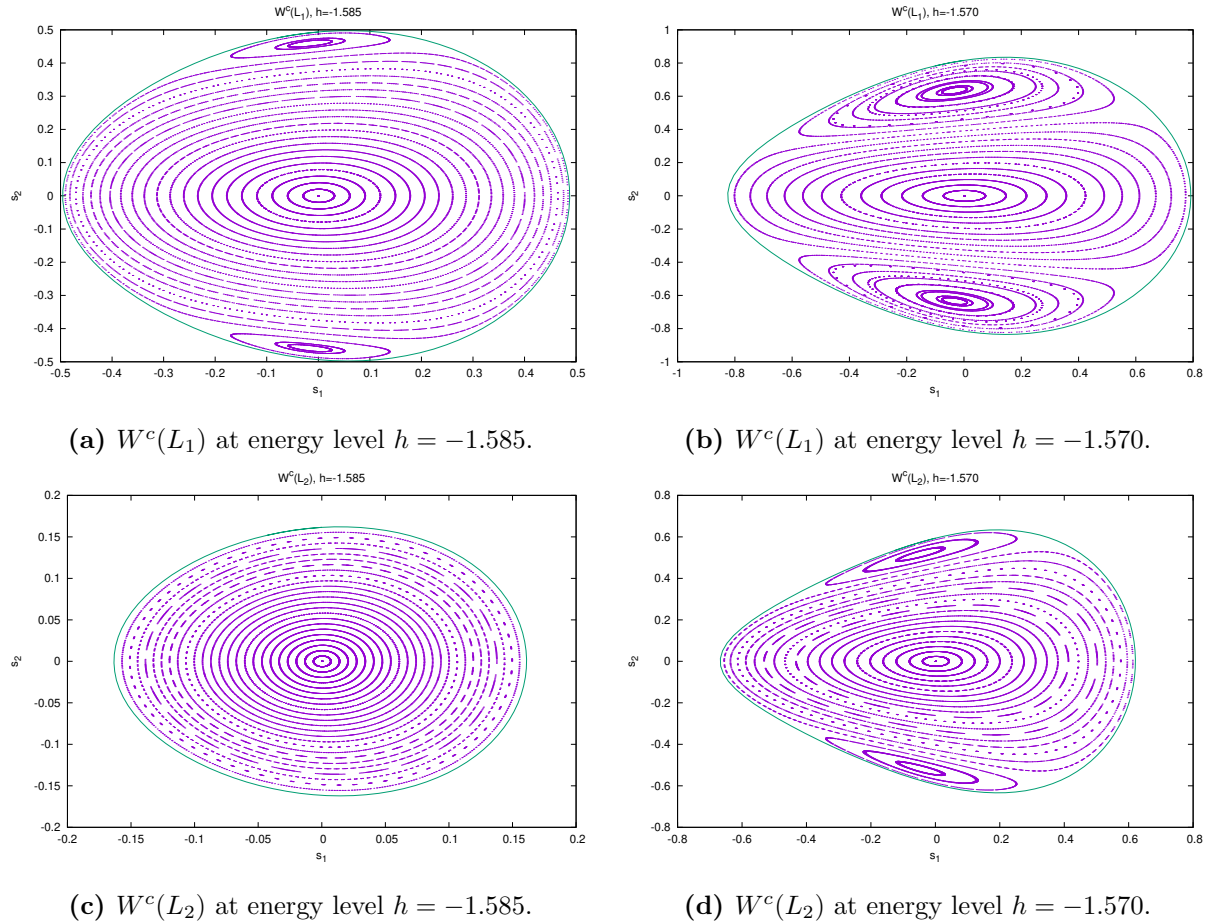


Figure 3.1: Poincaré sections at $\Sigma_h = \{s_4 = 0\}$ of $W^c(L_1)$ and $W^c(L_2)$ for two fixed levels of energy -1.580 and -1.570 of the Earth-Moon RTBP. The parameterizations are all computed using a mixed style with $I_1 = \{1, 2\}$ and $I_2 = \{3, 4\}$ and up to a maximum order 12.

3.1.1 Error Estimation

Our next goal consists on determining the domain of validity of the expansions for W^c using the e_O error estimation. This validity needs to be done for several energy levels and for different orders of the expansions of the center manifold in order to determine the quality of them. For that reason we need to choose the right initial conditions on the center manifold and a consistent time T_h of integration to compute the maximum error in the orbit at each order of computation and for each valid energy value h .

The computed Poincaré sections in Figure 3.1 represent only the intersections of the

10	20	30	40
24.371	389.286	2407.5	9274.6

Table 3.1: For several orders, computing times (in seconds) of an iso-energetic slice of $W^c(L_2)$ at $h = -1.585$ by taking 50 initial conditions in the s_2 axis and computing 100 Poincaré sections. The results are obtained on an AMD Ryzen 7 @ 2208.649Mhz.

10	20	30	40
3.394	51.455	304.61	1196.0

Table 3.2: For several orders, computing times (in seconds) of a set of points S_h from $W^c(L_2)$ at $h = -1.580$ and S_h made of 19641 points. The results are obtained on an Intel(R) Xeon(R) CPU E5-2630 v3 @ 2.40GHz by using multi-threaded computation and 16 threads.

trajectories starting from points of the form $(0, s_2, s_3, 0)$ with s_2 bounded by the planar Lyapunov orbit. However, for efficiency reasons, we would take as initial conditions a grid of equally spaced points over the Poincaré section Σ_h contained inside the planar Lyapunov orbit for a given energy value h at W^c . To do that, we choose a grid of points bounded by a square defined by the maximum and minimum s_1 and s_2 values of the planar orbit. Then, given a point in the square, we need to determine if it is inside or outside the considered region. In this way, we compute its angle θ respect the s_1 axis and its distance R to the origin. Therefore, if we take the corresponding point of the planar orbit at the same angle θ and at distance R_p from the origin, the given point will be inside the bounded region if $R < R_p$. However, since the planar orbit is computed by numerical integration, it is not always possible to get a point on the curve at the exactly given angle θ . To compute this point we proceed by polynomial interpolation by using Lagrange polynomials of degree 4.

Taking all of these into account, a set of n equally spaced points over the Poincaré section Σ_h is obtained. Next, we integrate them using reduced dynamics until their second intersection with Σ_h . Over all of these trajectories starting from the grid we take n_p points and hence we have a set S_h made of $n \times n_p$ points over the 4-dimensional manifold of $L_{1,2}$ that represents a significant sample of the center manifold. In Table 3.2, the computed times that are necessary to obtain these sets of points S_h for several orders are presented. Notice that these times increase in a non linear way as the order of the expansions is increased. In this case, the greater part of the computational effort is focused on the numerical integration of the expansions starting from the grid of n points over the Poincaré section Σ_h until the second intersection with Σ_h .

Finally, by choosing as the integration time T_h for the error in the orbit e_O the maximum of the periods of the planar and vertical Lyapunov periodic orbits of energy h , we compute the value of $e_O(T_h, \mathbf{s})$ for all the points $\mathbf{s} \in S_h$. Figure 3.2 shows the maximum $\epsilon(T_h, S_h)$ value in a logarithmic scale of all the computed $e_O(T_h, \mathbf{s})$ at each energy level and for different orders of the expansions. As we can see, for small energy values, the obtained improvement by increasing the order of expansions is null as the observed error corresponds to the error made during the integration procedure. Both plots shows that the expansions computed at order 20 provides a precision of $\sim 10^{-6}$ up to energy -1.580 . The rest of the errors increase as the energy is larger and finally they all collapse.

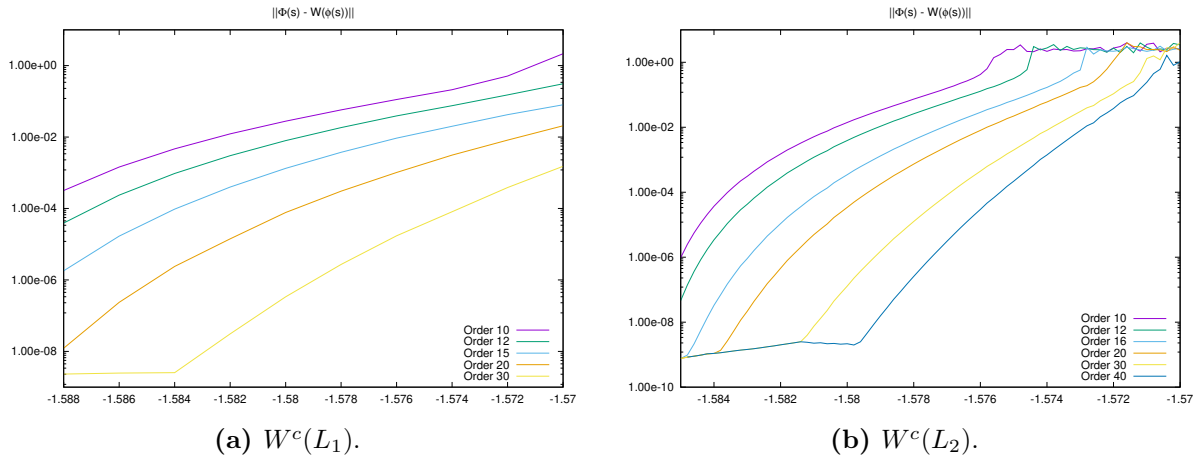


Figure 3.2: For the expansions of $W^c(L_1)$ and $W^c(L_2)$ for the Earth-Moon RTBP, computed up to orders indicated, evaluation of the maximum error estimate $\epsilon(T_h, S_h)$ for different energy values.

Lastly, for some energy values of h , the error $e_O(T_h, \mathbf{s})$ is represented in terms of the initial condition \mathbf{s} for all the points in the set S_h such that $s_4 = 0$. This means that the point \mathbf{s} belongs to the computed grid on the Poincaré section Σ_h . The Figure 3.3 shows the variation of the error in terms of the initial conditions on the 2D Poincaré section for the center manifold of L_1 and L_2 in a logarithmic scale. Both results are computed up to order 20 for the energy levels -1.585 and -1.578 using the expansions for L_1 and L_2 respectively. As we know for the plots in 3.2, these expansions give us a precision by 10^{-4} . However, Figure 3.3a only shows errors e_O less than approximately 10^{-7} . This means that the obtained $\epsilon(T_h, S_h)$ corresponds to a point \mathbf{s}_i with $s_4 \neq 0$, this \mathbf{s}_i is obtained through one of the trajectories starting at Σ_h . Another significant thing that is displayed in Figure 3.3 is that the error made in the expansions is not homogeneous over the Poincaré section $\{s_4 = 0\}$, but the larger errors are obtained on the outer initial conditions inside the region bounded by the planar Lyapunov orbit. Notice that the error estimations from [15], that are obtained by choosing initial conditions just on the s_2 axis, turn out to be too optimistic.

3.2 Computation of the Center-Stable and Center-Unstable Manifolds

We have seen how the parameterization method can be used to compute the center manifold of the collinear libration points L_1 and L_2 . By changing the way of choosing the set of indexes the value of d and the matrix \mathbf{P} , it can be used as well to compute the center-stable and center-unstable manifolds of those fixed points. On the one hand, the center-unstable manifold $W^{cu}(L_{1,2})$ of any of these libration points is an invariant manifold

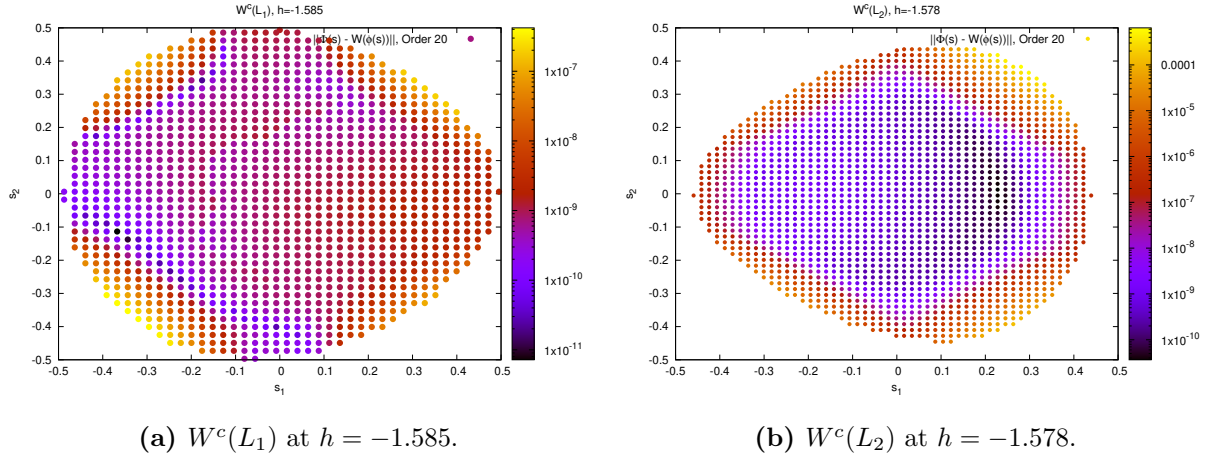


Figure 3.3: For the expansions of $W^c(L_1)$ and $W^c(L_2)$ for the Earth-Moon RTBP, computed up to order 20 and for the indicated energy level, evaluation of the error in the orbit $e_O(T_h, \mathbf{s})$ for all the points $\mathbf{s} \in S_h$ such that $s_4 = 0$.

that is tangent to eigenspace spanned by the eigenvectors with eigenvalues

$$i\omega_p^{1,2}, -i\omega_p^{1,2}, i\omega_v^{1,2}, -i\omega_v^{1,2}, \lambda^{1,2}, \quad (3.4)$$

while on the other hand, the center-stable manifold $W^{cs}(L_{1,2})$ is tangent to the directions given by the eigenvectors with eigenvalues

$$i\omega_p^{1,2}, -i\omega_p^{1,2}, i\omega_v^{1,2}, -i\omega_v^{1,2}, -\lambda^{1,2}. \quad (3.5)$$

Note that we have recovered the notation in (3.1) but adding the superscript 1, 2 according to which libration point they belong.

So, in order to get a parameterization of the 5D center-unstable manifold of L_2 and the 5D center-stable manifold of L_1 we proceed by taking $d = 5$ and $n = 6$ with the correct choice of the matrix \mathbf{P} depending on the manifold we want to compute. On the one hand, the matrix \mathbf{P} for the center stable-manifold will be made of the eigenvectors corresponding to the eigenvalues in (3.5), while on the other hand, the columns of \mathbf{P} for the center unstable-manifold have to be the eigenvectors of the eigenvalues in (3.4). Then, in order to adapt the dynamics in parameter space to get that s_1, s_2 are related with the planar Lyapunov family, s_3, s_4 to the vertical one, s_1, s_2, s_3, s_4 to the center manifold and s_5 with the normal hyperbolic part, we choose a mixed uncoupled style respect the s_5 coordinate with a set of $L = 3$ indexes [15]. This means that the reduced vector field needs to satisfy

that

$$\begin{cases} \dot{s}_1 &= f^1(s_1, s_2, s_3, s_4), \\ \dot{s}_2 &= f^2(s_1, s_2, s_3, s_4), \\ \dot{s}_3 &= f^3(s_1, s_2, s_3, s_4), \\ \dot{s}_4 &= f^4(s_1, s_2, s_3, s_4), \\ \dot{s}_5 &= f^5(s_1, s_2, s_3, s_4, s_5). \end{cases} \quad (3.6)$$

The set of indexes to generate the parameterizations and reduced vector fields of the invariant center-stable and center-unstable manifold of L_1 and L_2 of the RTBP for the Earth-Moon mass parameter is made of $I_1 = \{1, 2, 5\}$, $I_2 = \{3, 4, 5\}$ and $I_3 = \{5\}$. In this way, one obtains two parameterizations for W^{cs} and W^{cu} such that in any case $\{\bar{\mathbf{W}}(s_1, s_2, 0, 0, 0)\}_{s_1, s_2}$ describes the 2-dimensional manifold spanned by the planar Lyapunov family of orbits, $\{\bar{\mathbf{W}}(0, 0, s_3, s_4, 0)\}_{s_3, s_4}$ describes the 2D manifold corresponding to the vertical Lyapunov family of periodic orbits and $\{\bar{\mathbf{W}}(s_1, s_2, s_3, s_4, 0)\}_{s_1, s_2, s_3, s_4}$ corresponds to the center manifold of $L_{1,2}$ thanks to the choice of the indexes I_1 , I_2 and I_3 respectively.

Notice that we do not need to define an extra index set $I = \{1, 2, 3, 4\}$ that would made the points of the form $\{\bar{\mathbf{W}}(0, 0, 0, 0, s_5)\}_{s_5}$ to describe the normal hyperbolic part in all the objects of the center manifold. Since we use the mixed uncoupled style to get that s_1, \dots, s_5 are related with the center-stable (resp. center-unstable) manifold of L_1 (resp. L_2) by solving (3.6) and imposing that $\{s_5 = 0\}$ to be invariant then, automatically points of the form $\{\bar{\mathbf{W}}(0, 0, 0, 0, s_5)\}_{s_5}$ give the stable (resp. unstable) manifold of L_1 (resp. L_2). The mixed uncoupled style can be applied since, for $i = 1, \dots, 4$, it is satisfied that

$$\lambda_i - (m_1\lambda_1 + \dots + m_4\lambda_4 + m_5\lambda_5) \neq 0,$$

because $m_1\lambda_1 + \dots + m_4\lambda_4$ is a pure imaginary number while $m_5\lambda_5$ is always real and different from zero.

In this way, considering the reduced flow ϕ_t for the center-stable manifold of L_1 (resp. φ_t for the center-unstable manifold of L_2), by applying that $(s_1, s_2, s_3, s_4, s_5)$ represents the center stable manifold (resp. center-unstable) while (s_1, s_2, s_3, s_4) describes the center manifold because the choice of I_3 , one obtains that for any given point in parameter space such $(s_1, s_2, s_3, s_4, s_5)$ with $s_5 \neq 0$ it is satisfied that

$$\phi_t(s_1, \dots, s_5) \xrightarrow{t \rightarrow \infty} W^c(L_1) \quad (\text{resp. } \varphi_t(s_1, \dots, s_5) \xrightarrow{t \rightarrow -\infty} W^c(L_2)). \quad (3.7)$$

Therefore, thanks to the mixed uncoupled style which ensures that the first 4 components

10	20	30	40
15.096	343.91	3249.0	14525.286

Table 3.3: For several orders, computing times (in seconds) of a set of points S_h^2 from $W^{cu}(L_2)$ at $h = -1.580$ and S_h made of 19641 points. The results are obtained on an Intel(R) Xeon(R) CPU E5-2630 v3 @ 2.40GHz by using multi-threaded computation and 16 threads.

of $\phi_t(s_1, \dots, s_5)$ and $\phi_t(s_1, \dots, s_4, 0)$ are equal (resp. $\varphi_t(s_1, \dots, s_5)$ and $\varphi_t(s_1, \dots, s_4, 0)$) we have that

$$\|\phi_t(s_1, \dots, s_5) - \phi_t(s_1, \dots, s_4, 0)\| = \|\phi_t^5(s_1, \dots, s_5)\| \xrightarrow{t \rightarrow \infty} 0, \quad (3.8)$$

resp.

$$\|\varphi_t(s_1, \dots, s_5) - \varphi_t(s_1, \dots, s_4, 0)\| = \|\varphi_t^5(s_1, \dots, s_5)\| \xrightarrow{t \rightarrow -\infty} 0, \quad (3.9)$$

because the center manifold is given by $s_5 = 0$.

Consequently, (s_1, \dots, s_5) belongs to the fiber of (s_1, \dots, s_4) of the invariant stable (resp. unstable) manifold of the object that contains $(s_1, \dots, s_4, 0)$.

3.2.1 Error Estimation

Once the expansions for \mathbf{f} and \mathbf{W} are computed, we need to determine their domain of validity in terms of energy and the order of these expansions in a similar way to Section 3.1.1. However, we need to take now initial conditions with $s_5 \neq 0$ and integrate backward and forward in time in order to test both the stable and unstable center manifolds of L_1 and L_2 respectively. For that reason, for each center manifold and a given energy level h , we start by generating a set of points S_h^1 for L_1 and S_h^2 for L_2 using the same strategy as in Section 3.1.1 with the form $\mathbf{s} = (s_1, s_2, s_3, s_4, 0)$. Those points, as discussed above, belongs to center submanifolds belonging to the center-stable and center-unstable manifolds of L_1 and L_2 respectively. In this way, thanks to the decoupling of the last coordinate, we can modify the value of s_5 in each one of the points in S_h^i with $i = 1, 2$ and changing $s_5 = 0$ for a value δ and they still belong to the same energy value h .

The necessary computing times to obtain one of the S_h^i for $i = 2$ are presented in Table 3.3. In this case, compared to 3.2, the order 20 is almost as computationally expensive as the order 20 used to compute $W^c(L_2)$. This is due to the integration of one extra equation that appears with the choice of $d = 5$.

Consider the center-stable manifold of L_1 . With the choice of the eigenvector corresponding to $-\lambda^1$ we see that orbits with $s_5 < 0$ go from the vicinity of L_2 to the vicinity of L_1 [15]. While, by taking the center-unstable manifold of L_2 , the choice of the eigenvector

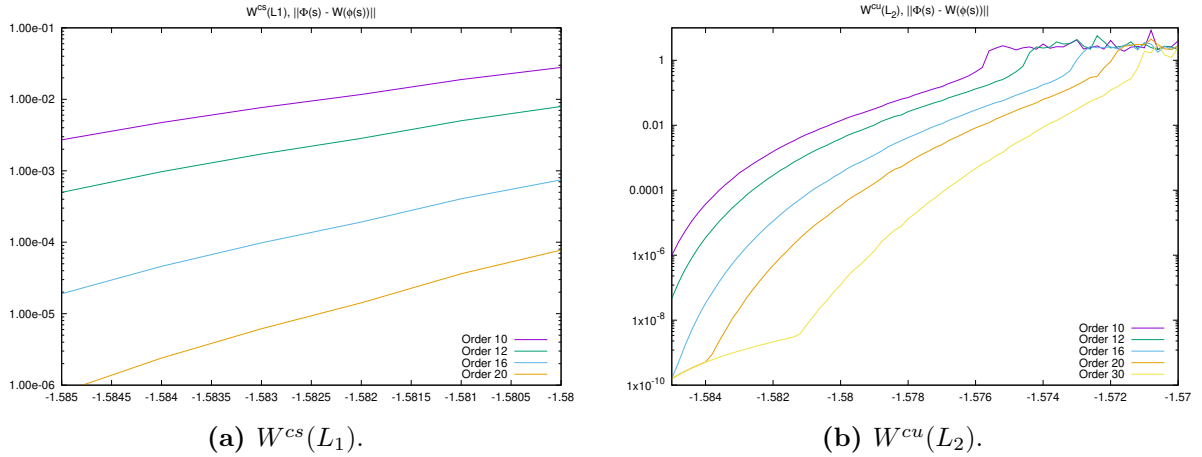


Figure 3.4: For the expansions of $W^{cs}(L_1)$ and $W^{cu}(L_2)$ for the Earth-Moon RTBP, computed up to orders indicated, evaluation of the maximum error estimate $\epsilon(T_h, S_h^i)$ for different energy levels and $s_5 = \pm 10^{-3}$ with $i = 1, 2$.

corresponding to λ^2 shows that the trajectories that come from the vicinity of L_1 correspond to points with the form $s_5 > 0$. Then, for a given energy value h , by choosing the integration time T_h to be the maximum of the periods of the planar and vertical Lyapunov orbits we integrate the points in S_h^1 backward in time and S_h^2 forward in time to determine the domain of validity of the expansions when approximating the corresponding invariant manifolds.

Let us take $\delta^1 = -10^{-3}$ for the expansion corresponding to $W^{cs}(L_1)$ and $\delta^2 = 10^{-3}$ for $W^{cu}(L_2)$. For these values, the maximum of the errors in the orbit $\epsilon(T_h, S_h^1)$ and $\epsilon(T_h, S_h^2)$ is computed for different energy levels and several orders for the expansions. In Figure 3.4 we present the obtained results for the indicated orders of the expansions in a logarithmic scale. Notice that the obtained errors are slightly larger than the ones resulting from the center manifold computation because one extra equation have been added. However, for expansions computed up to orders 20 and 30 we can ensure a precision of $\sim 10^{-5}$ up to energy -1.580 . In a similar way than we did in Section 3.1.1, we present the error in the center-stable and center-unstable manifolds in terms of the initial conditions \mathbf{s} restricted to the Poincaré section $\Sigma_h = \{s_4 = 0\}$ and the same value of δ^i for $i = 1, 2$. Again, the results shows that the error made is not homogeneous over the center manifold, but it is larger in the outer regions of the grid.

Notice that the range of energies used for the computation of the plot in 3.4a is selected in such a way that coincide with the energy ranges of $W^{cu}(L_2)$. In this case, the whole range of valid energies is not checked since the computational effort is high as we have seen in Table 3.3. In addition, we are interested on the study of heteroclinic connections so this analysis will be carried out for the same energy values that are valid in both libration points.

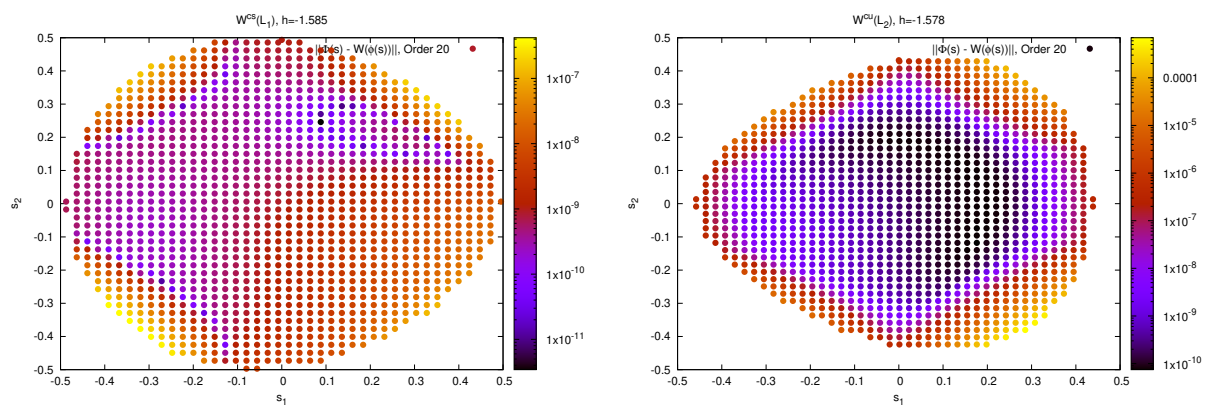
(a) $W^{cs}(L_1)$ at $h = -1.585$.(b) $W^{cu}(L_2)$ at $h = -1.578$.

Figure 3.5: For the expansions of $W^{cs}(L_1)$ and $W^{cu}(L_2)$ for the Earth-Moon RTBP, computed up to order 20 and for the indicated energy level, evaluation of the error in the orbit $e_O(T_h, \mathbf{s})$ for all the points $\mathbf{s} \in S_h$ such that $s_4 = 0$ and $s_5 = \pm 10^{-3}$.

Chapter 4

Numerical computation of heteroclinic connections

This chapter is focused on computing heteroclinic connections between the invariant tori around the L_1 and L_2 libration points of the Earth-Moon RTBP. An heteroclinic connection is a trajectory that links two different objects by tending backward in time to *the departure object* and forward in time to *the arrival object*. Besides, an homoclinic connection is a trajectory that connects an object with itself, meaning that tends to the same object backward and forward in time [14]. In the RTBP, these connections play an important role in terms of computing transfers between objects and mission analysis.

For a given dynamical system $\dot{\mathbf{x}} = \mathbf{X}(\mathbf{x})$ with an associated flow ϕ_t , let's consider a parameterization of the unstable manifold $W^u(K)$ for a given departure object K which is denoted by \bar{W}^u and the parameterization of the stable manifold $W^s(C)$ for a given arrival object C denoted by \bar{W}^s . Notice that these two objects could be the same in case we want to compute homoclinic connections. Then, let's take a Poincaré section given by $\Sigma_h := \{g(x) = 0\}$ for a given energy h and that it is intersected transversely by both of the manifolds. Let us also denote two time-return maps denoted by $\tau^+(x)$ and $\tau^-(x)$ to the Poincaré section. On the one hand, $\tau^+(x)$ is always positive and gives the time $t > 0$ to reach the Poincaré section by integrating forward in time. On the other hand, $\tau^-(x)$ corresponds to the time $t < 0$ to reach the Poincaré section and it is obtained by integrating backward in time.

Consequently, the two associated Poincaré maps to these manifolds are denoted by

$$P_{\Sigma^+}(\mathbf{x}) = \phi_{\tau^+(\mathbf{x})}(\mathbf{x}), \quad P_{\Sigma^-}(\mathbf{x}) = \phi_{\tau^-(\mathbf{x})}(\mathbf{x}), \quad (4.1)$$

where P_{Σ^+} results from the integration forward in time starting at K , whereas P_{Σ^-} is computed by integrating backward in time starting from C . In this way, these two sets

of points satisfy that $g(\phi_{\tau^+}(x)) = g(\phi_{\tau^-}(x)) = 0$ for all x in $W^u(K) \cup W^s(C)$. Note that the sub-index h at P_{Σ^+} and P_{Σ^-} is not included for the sake of notation simplicity.

Therefore, the intersections of homoclinic or heteroclinic connections with the Poincaré section Σ are given by the zeros of the following function [14],

$$F(\mathbf{s}^u, \mathbf{s}^s) = P_{\Sigma^+}(\bar{\mathbf{W}}^u(\mathbf{s}^u)) - P_{\Sigma^-}(\bar{\mathbf{W}}^s(\mathbf{s}^s)), \quad (4.2)$$

where \mathbf{s}^s is a point that belongs to the stable manifold and \mathbf{s}^u belongs to unstable manifold, both in terms of parameter space coordinates.

4.1 Determining Energies in Order to Look for Connections

As we have said before, our goal is to compute heteroclinic connections between the invariant tori from L_1 and L_2 . These tori are contained in the center manifold of L_1 and L_2 so we need to compute the stable and unstable manifolds these objects. But all the stable and unstable manifolds of invariant objects of the center manifold are contained in the center stable and center unstable manifolds of L_1 and L_2 respectively.

Therefore, we need to compute the center-stable and center-unstable manifolds of L_1 and L_2 respectively, so that the first one contains the arrival object and the second one the departure object. However, it is necessary to determine those energy levels for which heteroclinic connections can be observed and that are included in the domain of validity of the expansions for \mathbf{f} and \mathbf{W} . In our case, due to the cost of computation we select the order 20 for these expansions. This choice ensures that the computed expansions provide an approximation of the corresponding manifolds with a tolerance of 10^{-5} for any energy level between -1.586 and -1.584 in both libration points, as observed in 3.4. In this way, we start by computing the corresponding expansions $\bar{\mathbf{W}}^s$ and \mathbf{f}^s for the the center-stable manifold of L_1 , $W^{cs}(L_1)$, and $\bar{\mathbf{W}}^u$ and \mathbf{f}^u for the center-unstable manifold of L_2 , $W^{cu}(L_2)$. Both parameterizations are computed using the mixed uncoupled style and following the indications in 3.2.

Consider the planar Lyapunov orbits in $W^{cs}(L_1)$ and $W^{cu}(L_2)$ for different energies h and a Poincaré section given by $\Sigma_h := \{x = \mu - 1\}$ that is located between both libration points and particularly it is set at the same position on the x axis of the second primary, in this case the Moon. As we have seen in Section 3.1, the rest of the points of the iso-energetic slice of the Poincaré section $\{s_4 = 0\}$ of the center manifold will be contained inside the region defined by the planar Lyapunov orbit. The points that describes the planar Lyapunov orbits are of the form $\mathbf{s} = (s_1, s_2, 0, 0, 0)$ given by the choice of the

parameterization and as discussed in 3.2. By construction of the parameterization, these points are contained in the center manifold. It has also been seen that, in order to take into account only the trajectories that go from L_1 to L_2 and vice-versa, it is necessary to take the correct sign for the s_5 value. This means that we need to take the changes given by $s_5 = \alpha$ for the center-stable manifold of L_1 with $\alpha < 0$, and $s_5 = \beta$ for the center-unstable manifold of L_2 with $\beta > 0$.

Consider an initial condition from the planar Lyapunov orbit with the form $(0, s_2, 0, 0, 0)$ that it is obtained as discussed in 3.1. The integration until T_h , which is the period of this orbit, by using the reduced flow ϕ_t gives a set of n points of the form $(s_1, s_2, 0, 0, 0)$ that belongs to the center manifold. These points describe the planar Lyapunov orbit in $W^{cs}(L_1)$ and $W^{cu}(L_2)$ respectively and are obtained from $\phi_{iT_h/n}(0, s_2, 0, 0, 0)$ for $j = 0, \dots, n-1$. Therefore, by applying the change in the s_5 coordinate, we obtain two sets of points denoted by $\mathbf{s}_\delta^{1,i} = (s_1^i, s_2^i, s_3^i, s_4^i, \delta)$ the ones from $W^{cs}(L_1)$ and $\mathbf{s}_\delta^{2,i} = (s_1^i, s_2^i, s_3^i, s_4^i, \delta)$ the ones from $W^{cu}(L_2)$ for $i = 1, \dots, n$. After that, we apply the respective expansions for the parameterization to all of these n points. In this way, we obtain the following points in the original space $\{\bar{\mathbf{W}}^s(\mathbf{s}_\alpha^{1,i})\}_{i=1,\dots,n}$ and $\{\bar{\mathbf{W}}^u(\mathbf{s}_\beta^{2,i})\}_{i=1,\dots,n}$ for $\alpha = -10^{-3}$ and $\beta = 10^3$. Then, the intersection with Σ_h is computed by integrating in the original space of coordinates backward and forward in time. Therefore the sets $C_1 = \{P_{\Sigma^-}(\bar{\mathbf{W}}^s(\mathbf{s}_\alpha^{1,i}))\}_i$ and $C_2 = \{P_{\Sigma^+}(\bar{\mathbf{W}}^u(\mathbf{s}_\beta^{2,i}))\}_i$ for $i = 1, \dots, n$ are obtained.

Both the planar Lyapunov orbits and their invariant manifolds satisfy $z = p_z = 0$. Therefore, their heteroclinic connections can be computed in the planar RTBP, so we only need to consider the coordinates x, y, p_x, p_y . At Σ_h , the intersections of the trajectories that come from L_1 and the ones from L_2 have the same value of $x = \mu - 1$. There is another component that can be determined from the selected energy, in this case let it be the component p_x . Therefore, the computation of connections is reduced to determine those points $\mathbf{p}^s = (x^s, y^s, z^s, p_x^s, p_y^s, p_z^s) \in C_1$ and $\mathbf{p}^u = (x^u, y^u, z^u, p_x^u, p_y^u, p_z^u) \in C_2$ with $y^u = y^s$ and $p_y^u = p_y^s$.

The manifold tubes of the planar Lyapunov orbits around L_1 and L_2 are visualized in Figure 4.1 and also their intersections with Σ_h for three different energy levels and using expansions computed up to order 20. Note that the computation of P_{Σ^+} represents the fifth cut with Σ as we have seen by numerical exploration that the two manifold tubes do not intersect in the plane $x - y$ for any number of cuts less than the selected. Right figures in 4.1 shows that at least there exists two heteroclinic connections for the given energy levels.

In the next section we look for heteroclinic connections between tori around L_1 and L_2 at the energies that we have just found that there are heteroclinic connections between the planar Lyapunov orbits. According to the representation of the center manifold presented

in 3.1, there exists tori that are arbitrarily close to the planar Lyapunov orbits and, therefore, there are heteroclinic connections.

4.2 Computation of Connections Between Tori

Once the energy levels for which exist heteroclinic connections are determined from the projections to the Poincaré section Σ of the planar Lyapunov orbits by following the Figure in 4.1, we search for connections between the tori in the center-stable and the center-unstable manifolds of L_1 and L_2 respectively. For doing that, we proceed in the same way as before, but now we consider the whole $W^{cs}(L_1)$ and $W^{cu}(L_2)$, in the sense that we need to compute the intersections of these two objects with the Poincaré section given by Σ_h at an energy level h .

Let's consider a set of n_s points S^s from the center-stable manifold around L_1 and another set of n_u points S^u from the center-unstable manifold around L_2 at an energy level given by $h = -1.585$. These points are denoted by $\mathbf{s}_\alpha^{1,i} = (s_1^i, s_2^i, s_3^i, s_4^i, \alpha)$ the ones from S^s and $\mathbf{s}_\beta^{2,j} = (s_1^j, s_2^j, s_3^j, s_4^j, \beta)$ the ones from S^u for $i = 1, \dots, n_s$ and $j = 1, \dots, n_u$. From Figure 4.1, we know that for this exact energy h there exist at least two heteroclinic connections. The two sets S^2 and S^s are computed by following the same method as in section 3.2 from the application of the mixed uncoupled style of parameterization. The method gives us the two expansions for the parameterizations $\bar{\mathbf{W}}^s$ and $\bar{\mathbf{W}}^u$ corresponding to the center-unstable and center-stable manifolds of L_2 and L_1 respectively. Again, the sign of s_5 is determined from the direction of the chosen eigenvector in order to get trajectories susceptible to connect L_1 and L_2 . In this way, the Poincaré maps P_{Σ^+} and P_{Σ^-} of these two sets of points are computed with $\Sigma_h = \{x = \mu - 1\}$ and P_{Σ^+} and P_{Σ^-} are the intersections in the original space of the trajectories after integrating forward and backward in time starting from $W^{cs}(L_1)$ and $W^{cu}(L_2)$ respectively. This means that, from S^s and S^u , two sets of points $M_1 = \{P_{\Sigma^-}(\bar{\mathbf{W}}^s(\mathbf{s}_\alpha^{1,i}))\}_i$ and $M_2 = \{P_{\Sigma^+}(\bar{\mathbf{W}}^u(\mathbf{s}_\beta^{2,j}))\}_j$ are obtained. M_1 and M_2 are points that are located at Σ_h in the original space of coordinates.

Therefore, in order to find the zeros of the function in (4.2), we can compute the minimum distances between the manifold tubes at the intersection for any point from the arrival object respect to the departure object and vice-versa. This is given by the functions

$$\begin{aligned} d_s(\mathbf{s}_\alpha^{1,i}) &= \min_{\mathbf{s}_\beta^{2,j} \in S^u} \text{dist} (P_{\Sigma^-}(\bar{\mathbf{W}}^s(\mathbf{s}_\alpha^{1,i})), P_{\Sigma^+}(\bar{\mathbf{W}}^u(\mathbf{s}_\beta^{2,j}))), \\ d_u(\mathbf{s}_\beta^{2,j}) &= \min_{\mathbf{s}_\alpha^{1,i} \in S^s} \text{dist} (P_{\Sigma^+}(\bar{\mathbf{W}}^u(\mathbf{s}_\beta^{2,j})), P_{\Sigma^-}(\bar{\mathbf{W}}^s(\mathbf{s}_\alpha^{1,i}))), \end{aligned} \tag{4.3}$$

for any $\mathbf{s}_\alpha^{1,i}$ in S^s and $\mathbf{s}_\beta^{2,j}$ in S^u . The results of this evaluation are plotted in Figure 4.2 for values of $\alpha = -10^{-3}$ and $\beta = 10^{-3}$. As we can see, there exist a region where this

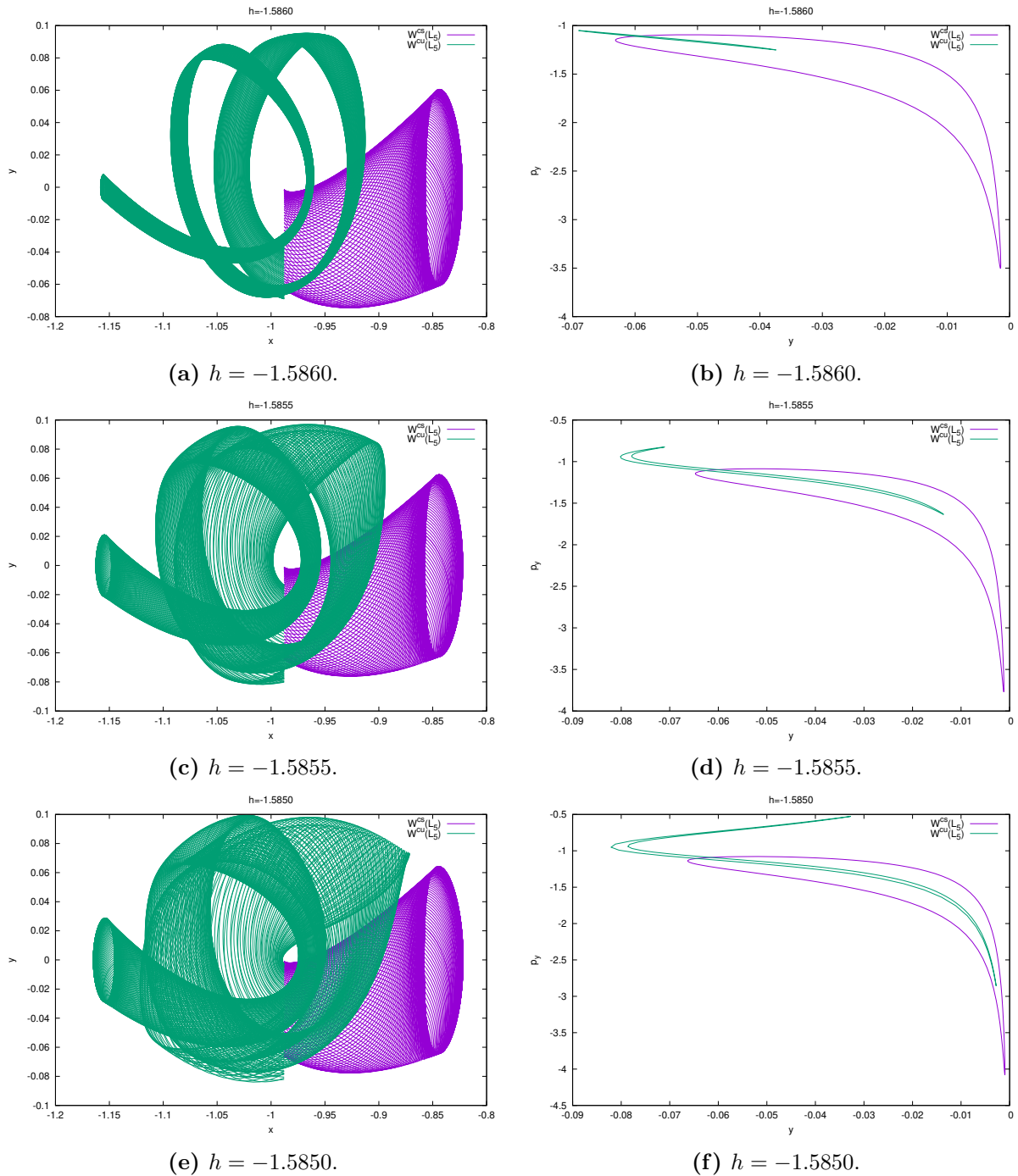


Figure 4.1: **Left:** manifold tubes (green: unstable, violet: stable) of a planar Lyapunov orbit around L_1 of the Earth-Moon RTBP using x and y coordinates. **Right:** intersection of the manifold tubes with the section $\Sigma_h = \{x = \mu - 1\}$ using y and p_y coordinates.

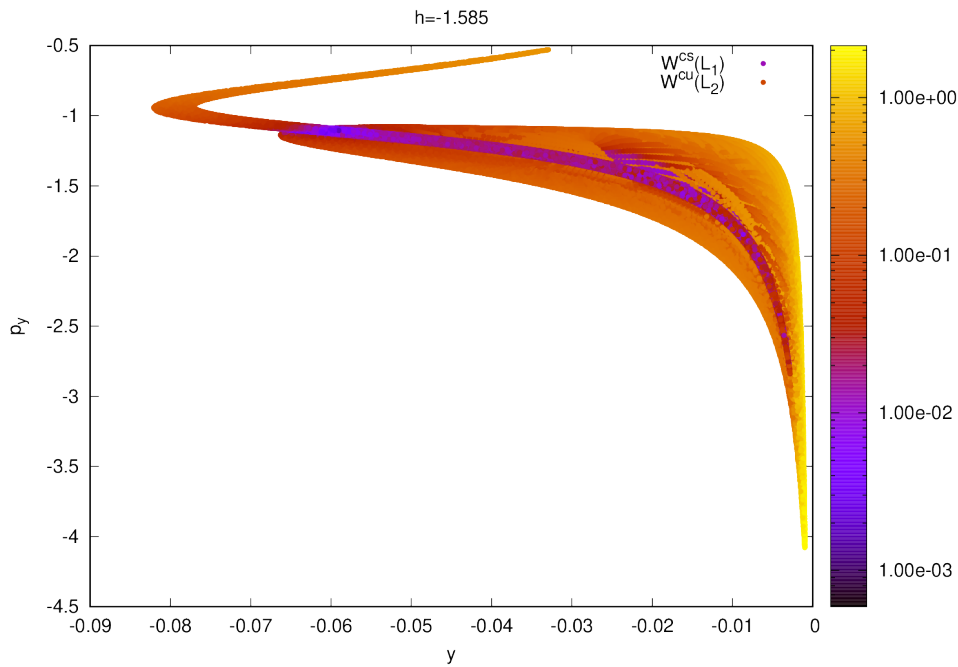


Figure 4.2: Intersection of the manifold tubes from $W^{cu}(L_2)$ and $W^{cs}(L_1)$ with the section $\Sigma_h = \{x = \mu - 1\}$ using y and p_y coordinates. It plots the minimum distance of each one of the points from one side respect to the other.

distance is minimum and could exist good candidates to become heteroclinic connections.

However, we need further information than the one provided by Figure 4.2 in order to compute these heteroclinic connections. For that reason we plot the same values obtained from (4.3) in terms of the initial conditions $\mathbf{s}_\alpha^{1,i}$ and $\mathbf{s}_\beta^{2,j}$ from $W^{cs}(L_1)$ and $W^{cu}(L_2)$ respectively. Figure 4.3 shows the projections of these initial conditions to the Poincaré section given by $\Omega_h := \{s_4 = 0\}$ at an energy level h . These plots show that exist zones inside the region bounded by the planar Lyapunov orbit that are more suitable to be the initial conditions to get heteroclinic connections. Nevertheless, due to the way of computing the sets of points S^s and S^u , these projections to Ω_h do not allow us to refine these sets in order to make zoom at these suitable regions. In our case, as we first compute a grid of points over the Poincaré section Ω_h and then we take the points after computing two Poincaré sections, we need to determine to which initial points over Ω_h belong the corresponding region of minimum distances. In this way, we plot in Figure 4.4 the minimum distances provided by (4.3) for all the points in S^s and S^u in terms of their retractions to the initial conditions over the grid of points taken at Ω_h before the numerical integration.

The plot in 4.4 shows that we can make a zoom over the Poincaré sections Ω_h in both $W^{cs}(L_1)$ and $W^{cu}(L_2)$ at the moment of the grid computation. By taking more initial conditions over the marked region, it is possible to get two other sets of points S^s and

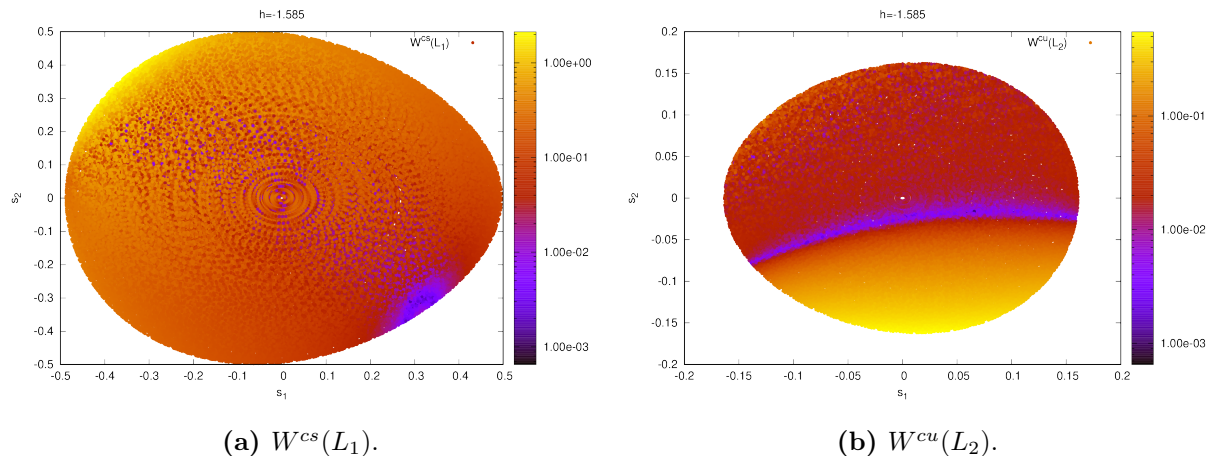


Figure 4.3: Projections of the initial conditions of $W^{cs}(L_1)$ and $W^{cu}(L_2)$ to the Poincaré section $\Omega_h := \{s_4 = 0\}$ in terms of the minimum distances given by (4.3) with $h = -1.585$.

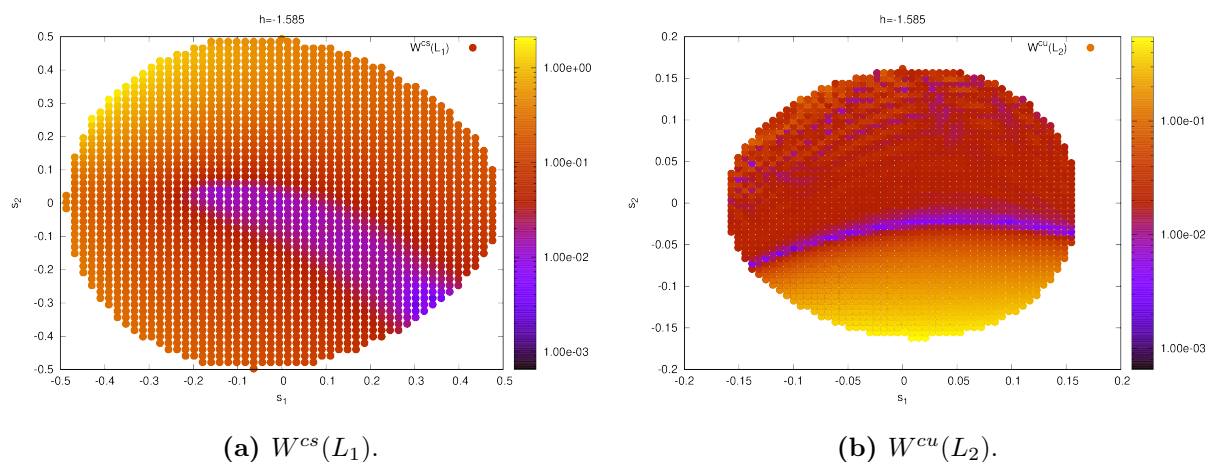


Figure 4.4: Retractions of the initial conditions of $W^{cs}(L_1)$ and $W^{cu}(L_2)$ to the grid of points over the Poincaré section $\Omega_h := \{s_4 = 0\}$ in terms of the minimum distances given by (4.3) with $h = -1.585$.

S^u from $W^{cu}(L_1)$ and $W^{cs}(L_2)$ in parameter space. With these new sets of points we compute again the sets M_1 and M_2 that corresponds to P_{Σ^+} and P_{Σ^-} . By checking all points of $P_{\Sigma^+}(S^u)$ against all points of $P_{\Sigma^-}(S^s)$, we can obtain pairs $\mathbf{s}^u \in S^u$, $\mathbf{s}^s \in S^s$ for which $\|F(\mathbf{s}^u, \mathbf{s}^s)\|$ is under a given tolerance, for F defined as in (4.2). These pairs provide heteroclinic connection candidates. With a tolerance of 10^{-3} , we get 4 different initial conditions in the center-stable manifold around L_1 and other 4 initial conditions in the center-unstable manifold around L_2 . We can integrate them forward and backward in time until the intersection with Σ_h starting from the arrival and the departure object respectively. By doing this, one obtains the trajectories displayed in Figure 4.5 that correspond to heteroclinic connections candidates since they are zeros of the function (4.2) within a tolerance set at 10^{-3} .

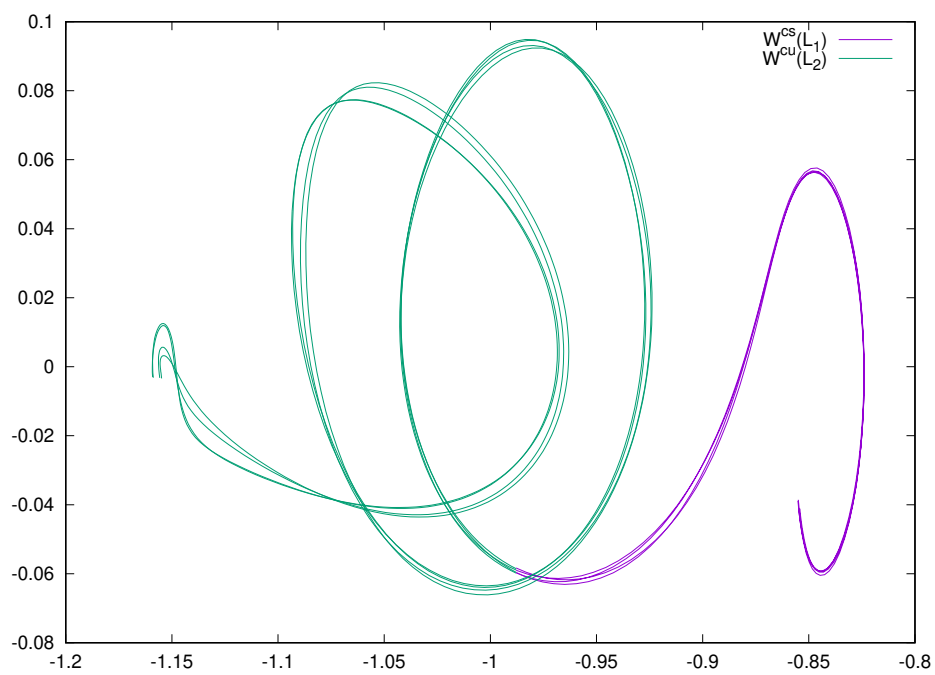


Figure 4.5: Heteroclinic connections corresponding to the zoom in 4.4 within a tolerance of 10^{-3} using x, y coordinates.

Conclusions

Once the analysis of heteroclinic connections between invariant tori around the two collinear libration points of the Earth-Moon RTBP has been carried out, there are few main points to be concluded.

The parameterization method provides a technique to reach for Taylor expansions of invariant manifolds around fixed points of flows and the corresponding reduced vector field. This method can be applied in order to obtain the center manifold, the center-stable manifold or the center-unstable manifold in different contexts of dynamical systems by choosing correctly the style of parametrization. The advantage of this method is related with the computational speed and also with its generality and flexibility in the sense that the implementation of the method is independent of the dynamical system and the coordinates of the manifold can be adapted to the dynamics by choosing a proper style of parameterization.

The implementation of one extra style of parameterization has been discussed: the mixed uncoupled style. This one allows the user to uncouple the first $d - 1$ coordinates of the reduced vector field respect to the last one. As we haven seen, this style is specially useful to compute the center-stable and the center-unstable manifolds.

In this way, an extensive representation of the central manifolds of both collinear libration points of the Earth-Moon RTBP has been carried out. These representations are also used to approximate the error in the manifold expansions that are obtained from the parameterization method with the correct way of choosing the style. This analysis of the error are more exhaustive than the ones that have been developed so far in the literature. This same exhaustive analysis of the error is also taken for the center-stable and center-unstable manifolds around these points by using the new mixed uncoupled style. The error analysis results, together with the ones of the center manifold, constitute one of the contributions of this work.

Finally, an analysis of heteroclinic connections between tori around collinear libration points is performed. This analysis uses the information obtained from the previous results in order to take into account the error in the expansions for different orders and depending on the energy level that it is studied. In this way, heteroclinic connections between planar

Lyapunov orbits have been found. Further, we have built an strategy to obtain a certain number of candidates of heteroclinic connections between these tori.

A natural continuation of this work would be to refine these candidates in order to get heteroclinic connections by solving numerically the equation (4.2) and using as initial guesses the obtained approximations that have been found in this project. Another way to get more accurate results would be to take more extensive zooms over the center manifold. However, due to the high computational cost related with the numerical integration of the reduced vector field, it would be convenient to explore other strategies that would allow us to obtain grids of points over the iso-energetic slices at the center manifold but avoiding the numerical integration.

Appendices

Appendix A

Comments on the Implementation

The computation of the numerical explorations that are included in this dissertation bases its programming core in the numerical routines that are included in the software package available in <http://www.maia.ub.edu/dsg/param/>. This software includes a C routine that computes expansions of invariant manifolds of fixed points of flows as described in Chapter 2. It also includes programs to evaluate the reduced field at the manifold from the obtained expansion for a given initial condition and to compute the change of the coordinates from parameter space to original space for any given initial condition in parameter space.

In addition, some other programs are provided by Josep-Maria Mondelo in order to manipulate dynamical systems. First of all, a routine that implements the Runge-Kutta-Fehlberg method of order 7 and 8 is given. This program is used in another routine that it is also provided and its function consists on computing the flow for a given vector field at a time t . Next, a routine to compute the Poincaré sections for a given a vector field, a set of initial conditions and a Poincaré section Σ is given. This routine is very useful to compute the intersection of the tubes included in Figure 4.1a, 4.1c and 4.1e. Finally, we receive a routine that computes the value of one of the components of any initial guess from parameter space in order to get an initial condition that satisfies a fixed energy. This is obtained from the implementation of a version corresponding to the Brent's Method included in [17]. This routine allows us to compute the initial conditions to get the iso-energetic slices in 3.1. Mondelo also assists in the development of a program to compute the minimum distance between two sets of points which is used in the results corresponding to Figures 4.2, 4.3 and 4.4.

The rest of the programs used to obtain the results included in the current project are original. They include the modification of the software package to provide tools in order to obtain the parameterization expansions corresponding to a mixed uncoupled style. This modification allows the user to uncouple the $d - 1$ first components from the last one and it is very useful when computing center-stable and center-unstable manifolds. It

is also developed a program to compute a grid of equally spaced points inside a region bounded by the planar Lyapunov orbit by looking for points that satisfy the given energy value. This program uses parallel routines from the library `omp.h` in order to reduce the computational time. This program includes some optional input arguments in order to make zooms inside the bounded region. These routines are complemented with a program focused on computing the error in the orbit from a set of initial conditions and a given expansion. These programs allow us to obtain the results included in Figures 3.2, 3.3, 3.4 and 3.5.

Bibliography

- [1] G. Gomez, M. W. Lo, and J. Masdemont, “Libration Point Orbits and Applications,” Singapore: World Scientific, 2003, 695.
- [2] T. H. Sweetser, S. B. Broschart, V. Angelopoulos, G. J. Whiffen, D. C. Folta, M. K. Chung, S. J. Hatch, and M. A. Woodard, “ARTEMIS mission design,” *Space Science Reviews*, **165**, 1-4, 27–57, 2011.
- [3] J. Llibre, R. Martínez, and C. Simó, “Transversality of the invariant manifolds associated to the Lyapunov family of periodic orbits near L2 in the restricted three-body problem,” *Journal of Differential Equations*, **58**, 1, 104–156, 1985.
- [4] G. Gómez and J. Masdemont, “Some zero cost transfers between libration point orbits,” in *AAS 00-177*, 2000.
- [5] G. Gómez, M. Marcote, and J. M. Mondelo, *The invariant manifold structure of the spatial Hill’s problem*, 1. 2005, vol. 20, 115–147.
- [6] L. Arona and J. Masdemont, “Computation of Heteroclinic Orbits Between Normally Hyperbolic Invariant 3-Spheres Foliated by 2-Dimensional Invariant Tori in Hill’s Problem,” *Discrete And Continuous Dynamical Systems*, 64–74, 2007.
- [7] E. Canalias and J. J. Masdemont, “Homoclinic and heteroclinic transfer trajectories between planar Lyapunov orbits in the Sun-Earth and Earth-Moon systems,” *Discrete and Continuous Dynamical Systems*, **14**, 2, 261–279, 2006.
- [8] E. Barrabés, J. M. Mondelo, and M. Ollé, “Numerical continuation of families of heteroclinic connections between periodic orbits in a Hamiltonian system,” *Nonlinearity*, **26**, 10, 2747–2765, 2013.
- [9] G. Gómez, W. S. Koon, M. W. Lo, J. E. Marsden, J. Masdemont, and S. D. Ross, “Connecting orbits and invariant manifolds in the spatial restricted three-body problem,” *Nonlinearity*, **17**, 5, 1571–1606, 2004.

-
- [10] A. Delshams, J. Masdemont, and P. Roldán, “Computing the scattering map in the spatial Hill’s problem,” *Discrete Contin. Dyn. Syst. Ser. B*, **10**, 2-3, 455–483, 2008.: <https://doi.org/10.3934/dcdsb.2008.10.455>.
- [11] D. K. Arrowsmith and C. M. Place, *An Introduction to Dynamical Systems*. New York, 1994.
- [12] S. Wiggins, *Introduction to applied nonlinear dynamical systems and chaos*. Telos: Springer, 1997.
- [13] V. Szebehely, *Theory of orbits*. Academic Press, Inc., 1967.
- [14] J.-M. Mondelo, “Computing Invariant Manifolds for Libration Point Missions,” in *Satellite and Space Missions*, G. Baù, A. Celletti, and G. Federico Gronchi, Eds., Springer, 2016.
- [15] A. Haro, M. Canadell, J.-L. Figueras, A. Luque, and J.-M. Mondelo, *The Parameterization Method for Invariant Manifolds*. Springer, 2010, 1–41.
- [16] K. R. Meyer, G. R. Hall, and D. Offin, *Introduction to Hamiltonian Dynamical Systems and the N-Body Problem*, 2nd. Springer-Verlag, 2009.
- [17] W. H. Press, S. A. Teukolsky, W. T. Vetterling, and B. P. Flannery, *Numerical Recipes in C*, 7. Cambridge University Press, 1992, vol. 76.